5 Results

5.1 Characterization of HEK293 cell clones stably expressing N-terminal FLAG-tagged wild-type and mutant V2Rs

5.1.1 Expression of the wild-type V2R

The study of degradation pathways of the human V2R required proteins tagged with immunoreactive epitopes to facilitate their biochemical characterization. The FLAG-tag, a small polypeptide protein tag that enables the purification and detection of recombinantly expressed fusion proteins, was placed by insertional PCR at the N terminus of the V2R (amino acid sequence position -8 to -1). The N-terminal FLAG-fusion should not influence intracellular signal transduction pathways, trafficking or pharmacological properties of the receptor.

First, HEK293 (human embryonic kidney, clone 293) cells were stably transfected with FLAG.V2R cDNA to achieve homogenous protein expression levels. During protein synthesis, the nascent V2Rs are inserted into the ER membrane and post-translationally modified with high-mannose glycosylation residues (core-glycosylation). Subsequently, correctly folded receptors begin a journey through the secretory pathway. The core-glycosylated receptors cross the ERGIC and are transported to the Golgi apparatus. Enzymes in the Golgi network substitute the high-mannose modifications with complex sugar moieties and additionally insert sugar chains at serine and threonine residues (O-glycosylation). The mature, fully-glycosylated receptors are exported to the plasma membrane, their final destination and site of action. For the identification of the type of glycoprotein (core- or complex-glycosylated form), a digestion with the glycosidases Endo H and PNGase F is a useful method, because it contributes to the characterization of intracellular localization of glycoproteins; the enzyme Endo H cleaves off high-mannose glycosylation forms linked to asparagine residues in the ER. Glycoproteins that reach at least the medium-Golgi become resistant to the action of Endo H through further additions of complex sugar moieties. PNGase F catalyzes the cleavage of all N-linked sugar chains, high-mannose- and complex-glycosylation. Thus, depending on the ability of Endo H and / or PNGase F to digest the proteins of interest, the location of the proteins in the secretory pathway can be determined.

For the analysis of the V2R expression, cells were lysed and the FLAG.V2R fusion proteins were immunoprecipitated by an immune-complex of protein A-Sepharose and an anti-FLAG M2 antibody. The precipitated receptors were divided into three equal parts

and were subjected to digestion with the glycosidases Endo H, PNGase F or left untreated. Subsequently, samples were analyzed by SDS-PAGE and western blot (Fig.1).

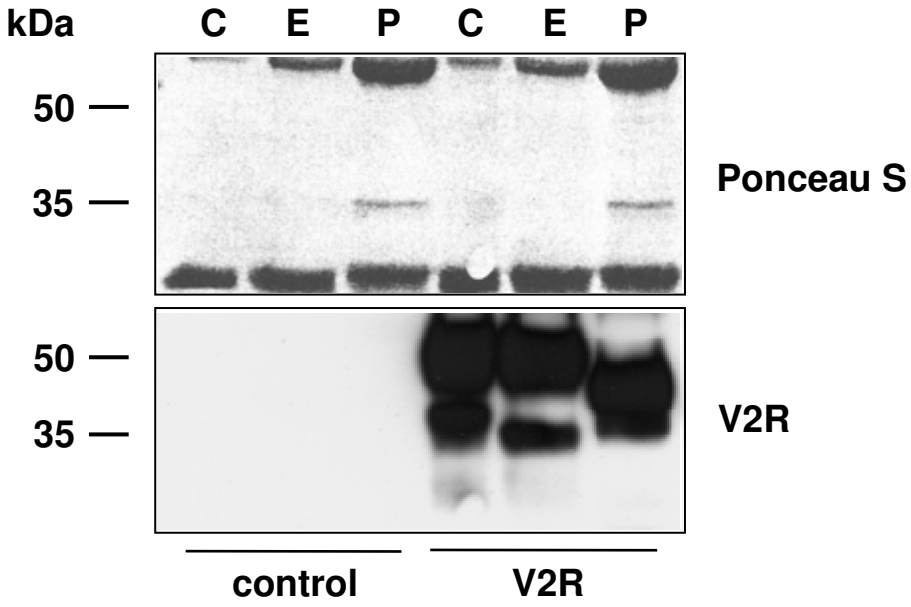

Fig. 1: Digestion of V2Rs with the deglycosylating enzymes Endo H and PNGase F. Confluent HEK293 cells stably expressing FLAG-tagged V2Rs were lysed and subjected to immunoprecipitation by an immune-complex of protein A-Sepharose and an anti-FLAG antibody. Receptor proteins were digested with Endo H (E), PNGase F (P) or without enzymes (C), separated by SDS-PAGE on 10 % acrylamide gels and subsequently immunoblotted. All proteins on the nitrocellulose membrane were stained with Ponceau S (*upper panel*). Receptors on the same membrane were detected by a mouse anti-FLAG antibody, a POD-conjugated secondary antibody and the ECL system (lower panel). Controls were untransfected HEK293 cells. Molecular weight markers are shown on the left. This blot is representative of five individual experiments.

The Ponceau S staining of the membrane revealed unspecific bands due to the precipitating antibody and the enzymatic reaction (the size of PNGase F is 36 kDa) (Fig. 1, *upper panel*). Controls for the experiments were non-transfected HEK293 cells. The detection of the receptors was carried out by a mouse monoclonal anti-FLAG M2 antibody (Fig. 1, *lower panel*). The V2R was expressed in two specific forms; the weak 38 kDa band showed the core-gycosylated immature receptor form (Fig. 1, *lower panel, C*) and the prominent, broad band running at 45 - 55 kDa represents the complex-glycosylated, mature receptors. Treatment with Endo H (Fig. 1, *lower panel, E*) reduced the size of the 38 kDa band (core-glycosylated receptors) to a 35 kDa band corresponding to non-glycosylated receptors. Digestion with PNGase F (Fig. 1, *lower panel, P*) led to a shift of both bands and to the detection of a new 42 kDa receptor type. The complex-glycosylated receptors did not reach the size of the non-glycosylated receptors, because the V2R is also O-glycosylated at serine and threonine residues in the Golgi apparatus. This O-glycosylation has been described by Sadeghi et al. and is resistant for both enzymes (Sadeghi and Birnbaumer 1999). The proteins isolated from untransfected HEK293 cells (control) revealed no detectable signals. This proves the purity of the

precipitation and the high specificity of the FLAG-antibody used for detection of receptor proteins.

Most of the V2Rs were expressed in the complex-glycosylated, mature form indicating that the FLAG-tag does not affect ER to Golgi transport. The receptors were localized in compartments after the cis-Golgi, probably at the plasma membrane. The minority of receptors were immature transport-intermediates due to newly synthesized, nascent receptors during the folding process or to improper folding.

5.1.2 Characterization of the saturation ligand binding activity of the wild-type V2R

The HEK293 cell line stably expressing FLAG-tagged V2Rs was tested for its specific hormone binding activity to ensure that the N-terminal FLAG-tag does not alter the pharmacological properties of the V2R and to analyze the level of receptor expression. In this assay the specific binding isotherm was calculated from the difference between the binding of distinct concentrations of [^{3}H]AVP in presence (total binding) and absence (unspecific binding) of unlabeled AVP to intact cells. After incubation with the ligands, the cells were washed, lysed and the bound [^{3}H]AVP was measured in a scintillation counter. The saturation binding activity was analyzed with the Prism GraphPad software (version 3.0). The dissociation constant (K_D) and maximal binding (B_{max}) were calculated from the resulting specific binding isotherms.

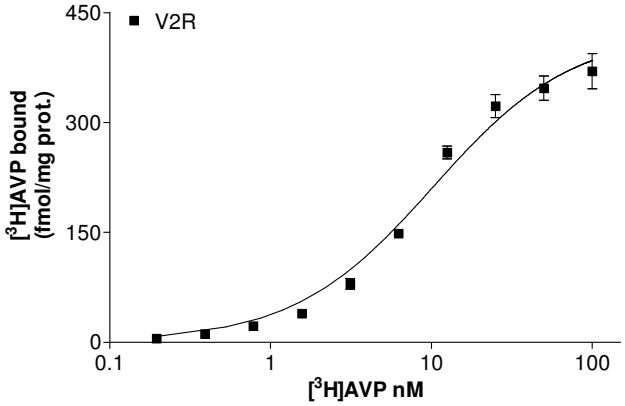

Fig. 2: Pharmacological characterization of FLAG-tagged V2R constructs. Specific [^{3}H]AVP binding isotherm for HEK293 cells stably expressing FLAG-tagged wild-type V2R. Data represent mean values of triplicates, which differed by less than 5 %. In all binding experiments, unspecific binding contributed up to 30 % of total binding. SEM are depicted. The results are representative of three individual experiments. Triplicates differed by less than 10 %. SEM are depicted.

Figure 2 depicts a representative binding profile. The wild-type V2R had a calculated K_D of 10.24 ± 1.42 nM and a B_{max} of 424.10 ± 18 fmol / mg protein (Fig. 2), computed as mean values of three independent experiments. Comparison with parameters reported by others in transiently transfected cells revealed a small decrease in the receptor affinity to AVP.

plasmid	K_D (nM)	B_{max} (fmol/mg protein)	literature
FLAG.V2R	10.24 ± 1.42	424.10 ± 18	Present work
V2R (HEK)	5.0 ± 0.5	-	(Gouill, Darden et al. 2005)
V2R.GFP (HEK)	1.97 ± 0.37	697 ± 62	(Hermosilla, Oueslati et al. 2004)
HA.V2R (COS)	2.5 ± 0.3	- (355 fmol / well)	(Innamorati, Sadeghi et al. 1996)
V2R (COS)	3.6 ± 1.9	530 ± 155	(Oksche, Leder et al. 2002)

5.1.3 Adenylyl cyclase (AC) activity induced by the wild-type receptor

The function and signaling properties of the receptor were analyzed by its ability to activate adenylyl cyclases. The AC assay measures the formation of radiolabeled [^{32}P]cAMP after stimulating the AC system, either directly by forskolin or via a receptor that couples to G_S proteins. Crude membrane fractions of HEK293 cells stably expressing the FLAG-tagged wild-type receptor were isolated and 20 mg of protein were subjected to the assay. Adenylyl cyclase activity was induced by stimulation with different concentrations of AVP (from 0.03 to 1000 nM) or by 100 µM forskolin. After isolation of the generated [^{32}P]cAMP by column chromatography, the radioactivity was measured in a scintillation counter. Mean values were calculated and the adenylyl cyclase activity was normalized to the forskolin-response (100 %). The curve was constituted as the percentage of the maximal response using logarithmic AVP concentrations with the Prism GraphPad software (vision 3.0). The curve of the mean values is shown in figure 3. The EC50 (half maximal effective concentration) was assessed from the curve by the iterative calculation procedure for non-linear regression analysis. The EC50 of the V2R was 73.90 + 0.19 nM (Fig. 3) and is in agreement with data published by others.

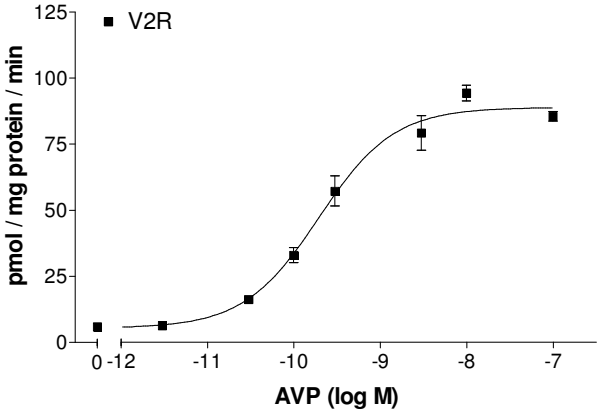

Fig. 3: AC assay of HEK293 cells stably expressing the wild-type V2R. Adenylyl cyclase activity assays were performed with crude membranes of stably transfected HEK293 cells expressing the FLAG-tagged wild-type V2R. Data represent mean values of three independent experiments each performed in triplicate. Triplicates differed by less than 10 %. SEM are depicted.

5.1.4 Activation of the MAPK signaling cascade

It has been demonstrated that stimulation of the V2R leads to activation of the MAPK signaling pathway by a β-arrestin-dependent mechanism (Charest, Oligny-Longpre et al. 2007). The authors propose that the AVP-induced V2R signaling activates the Raf – MEK1/2 - ERK1/2 cascade. Serum-starved HEK293 cells stably expressing the FLAG-tagged V2R were analyzed for the ability to activate ERK1/2 with different ligand concentrations (Fig. 4). Total cell lysis was performed and equal amounts of proteins were separated by SDS-PAGE. Incubation with 10 nM AVP for 10 min was sufficient to detect the active, phosphorylated forms of ERK1 and ERK2 at 42 and 44 kDa, respectively. Higher AVP concentrations lead to a broad increase in ERK phosphorylation (Fig. 4, *upper panel*). Between 500 nM and 1000 nM AVP, there was no further enhancement of the signals of phosphorylated ERK, which indicated maximal ERK activation. The unphosphorylated forms of ERK1/2 served as loading controls and demonstrated that equal amounts of proteins were utilized in the assay (Fig. 4, *lower panel*). The results indicate that activation of the V2R with 10 nM of AVP is sufficient to initiate MAPK signaling.

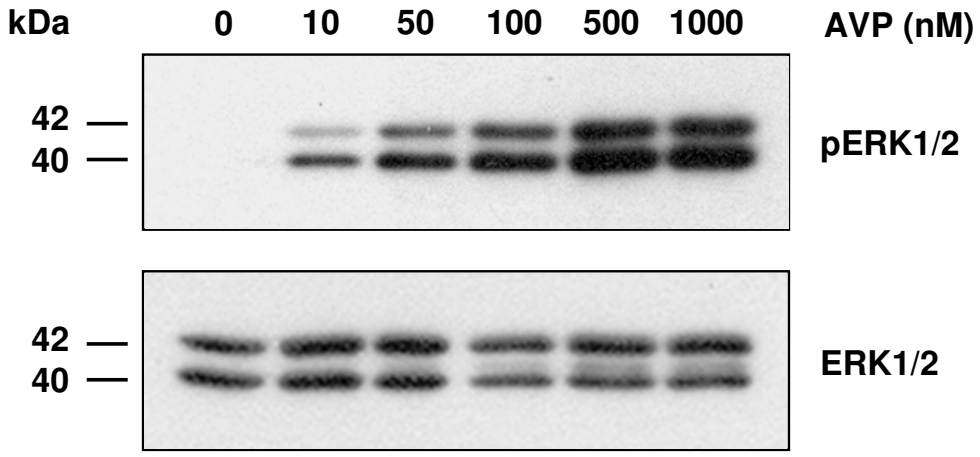

Fig. 4: ERK1/2 activation mediated by the wild-type FLAG.V2R. HEK293 cells stably expressing the FLAG.V2R were treated with the indicated amounts of AVP for 10 min. Total cell lysis was performed and equal amounts of proteins were separated by SDS-PAGE, immunoblotted and proteins were detected with a polyclonal rabbit anti-p42 / 44 MAP kinase (ERK1/2) and a polyclonal rabbit anti-phospho p42 / 44 MAP kinase IgG (pERK1/2). Blots were developed with a POD-conjugated secondary antibody and the ECL system. The blots are representative of three individual experiments.

5.1.5 Internalization of activated V2Rs to lysosomal structures

The inactive wild-type V2R is mainly localized at the plasma membrane, but a small amount of receptors is also described to be located in endosomal structures (Robben, Knoers et al. 2004). For the study of receptor internalization, a HEK293 cell line stably expressing V2R.GFP fusion proteins was investigated with a confocal laser-scanning microscope (Fig. 5). The cells were left untreated (*upper panel*) or incubated with 1 µM

AVP for 10 min (*lower panel*) to achieve maximal stimulation. GFP fluorescence was visualized in the green channel, the receptors revealed a prominent membrane localization. In presence of AVP more receptors were located in vesicular structures in the cytoplasm and the membrane fluorescence signals decreased. Lysosomal vesicles were dyed with 150 nM of the fluorescent marker Lysotracker (red channel) and an overlay of both channels was computed. The co-localization signals of receptors and lysosomes increased under hormone stimulation. These results confirm that the agonist-stimulated V2R is internalized into a lysosomal compartment. According to the work of Robben et al., they also revealed co-localization of receptors and lysosomes at steady state.

Data demonstrated by Martin et al. showed an increase in polyubiquitin signals of ligand-activated V2Rs during internalization (Martin, Lefkowitz et al., 2003), this result could be confirmed in this thesis (see App. Figure 6).

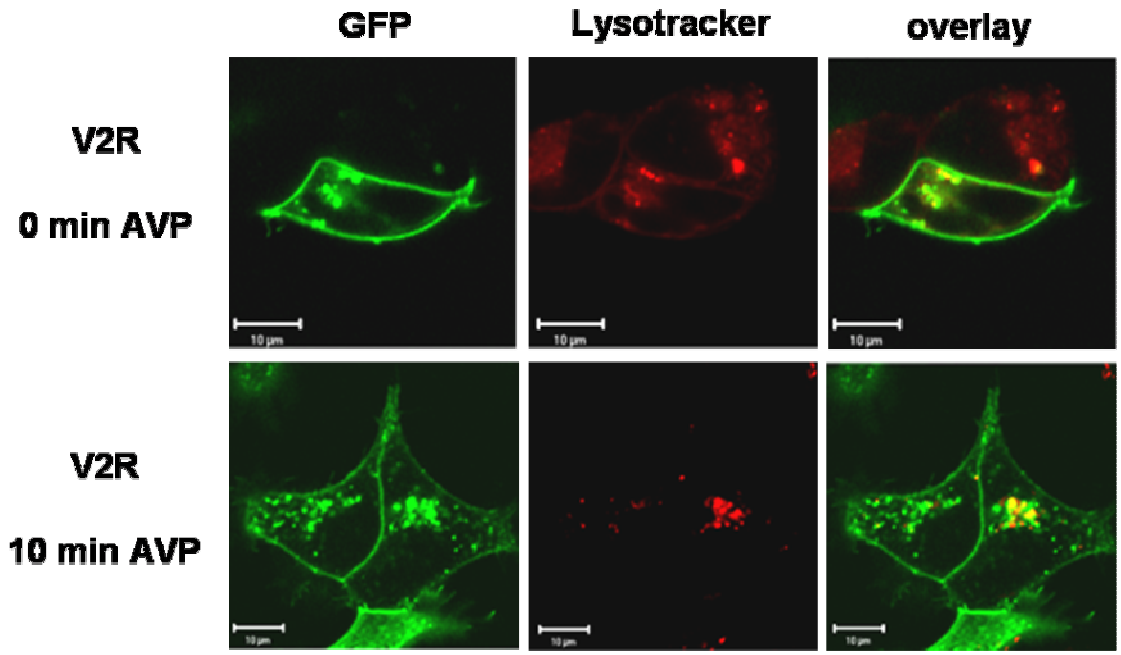

Fig. 5: Lysosomal localization of AVP-activated wild-type V2Rs. HEK293 cells stably expressing GFP-tagged wild-type V2Rs were incubated with 150 nM of the lysosomal marker Lysotracker and treated with 1 µM AVP for 10 min. The cells were analyzed by confocal laser-scanning microscopy with horizontal (*xy*) scans before and after stimulation with AVP. Receptor fluorescence signals are shown in green (left panels) and Lysotracker signals of the same cells in red (central panels). Both fluorescence signals were computer-overlaid (right panels; overlap is indicated by yellow). The scans show representative cells. Scale bar, 10 µm. Similar data were obtained in three independent experiments.

5.1.6 Localization of three NDI-causing mutant V2Rs in the early secretory pathway

The cellular quality control system is responsible for the export of correctly folded receptor proteins from different compartments of the secretory pathway. If the V2Rs fail

the quality control due to mutations in the *AVPR2* gene and subsequent folding defects in their three-dimensional structure, mutated receptors are retained in these compartments, are hindered in their cell surface expression and therefore cause NDI. To access the fate of such retained proteins, three receptors with mutations in different receptor domains located in distinct intracellular retention compartments were chosen for the study. All investigated NDI-causing mutants of the receptor originated from point mutations leading to single amino acid exchanges (see introduction, Figure 6). The L62P mutation is presumably localized at the interface between the first transmembrane region and the first intracellular loop (cytosolic). The mutant is retained in the ER exclusively. The G201D amino acid exchange occurs in the second extracellular loop; the mutation causes Golgi apparatus retention (luminal). Some receptors bearing the G201D mutation are able to evade the quality control mechanisms and are also expressed to some extent at the plasma membrane. The S167L and V226E mutations lay in the forth and fifth transmembrane region, respectively. S167L mutants are located in the ER, whereas V226E mutants are reported to be retained in the ERGIC (Hermosilla, Oueslati et al. 2004). In the present work, the cDNAs of all mutant receptors were generated by site-directed mutagenesis out of FLAG.V2R as a template and the resulting mutant receptor constructs were stably transfected in HEK293 cells. The survival of the stably expressing cell lines was the first indication of adaptation by the cells to the stress caused by the intracellular retention of misfolded V2R.

To date, the different retention compartments described in the literature were determined with GFP-tagged V2Rs. To verify that the FLAG-tag does not affect the intracellular localization, immunofluorescence staining of paraformaldehyde fixed HEK293 cells stably expressing the mutant receptors was performed as described in “Materials and Methods” and analyzed on a confocal laser-scanning microscope. The cell membranes of the fixed cells were permeabilized by detergents so that receptors and intracellular compartments could be stained with specific antibodies. The receptors were detected by an anti-FLAG antibody (mouse or rabbit) and dyed by an anti-mouse or an anti-rabbit antibody coupled to cyanine 3 (Cy3), respectively (Fig. 6, *green channel*). Intracellular compartments were visualized with compartment specific antibodies (ER: calnexin, ERGIC: ERGIC-53 in presence of bafilomycin A1, Golgi apparatus: GM130) (Fig. 6, *red channel*) and an overlay of both channels was computed.

The FLAG-tagged wild-type V2R was predominantly located at the cell membrane (Fig. 6, *upper panel*). In contrast to the wild-type, mutant L62P showed a typical ER distribution pattern (Fig. 6, *middle panels*). The receptors were diffusely localized in cytoplasmic structures excluding the nucleus. The ER was identified by the ER membrane-bound protein calnexin, which is expressed in the ER exclusively. L62P and calnexin signals showed co-localization in intracellular structures confirming the ER retention of mutant L62P.

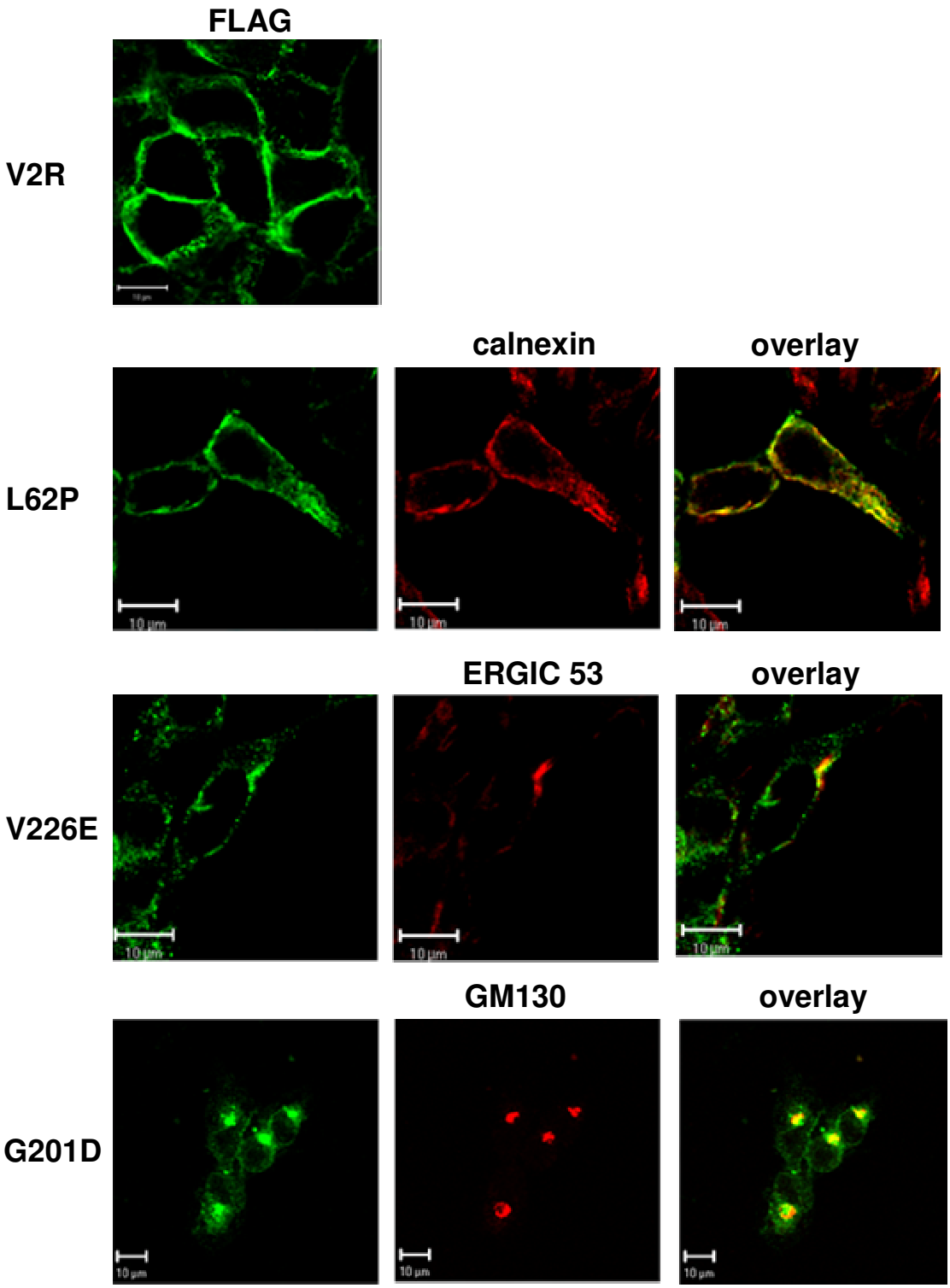

Fig. 6: Subcellular localization of FLAG-tagged wild-type and mutant V2Rs in stably expressing HEK293 cells. Cells expressing the receptor mutant V226E were pretreated for 4 h with bafilomycin A1. Cells expressing the wild-type V2R and receptor mutants L62P, V226E, and G201D were fixed and permeabilized. They were incubated with a monoclonal mouse α-FLAG antibody. G201D was detected with a polyclonal rabbit α-FLAG antibody. A simultaneous staining of specific compartments was carried out (for L62P, calnexin; for V226E, ERGIC-53; for G201D, GM130). The secondary antibodies were in all cases an Alexa Fluor® 488 goat α-rabbit IgG and a goat α-mouse Cy3 IgG. The samples were analyzed by confocal laser-scanning microscopy with horizontal (*xy*) scans. Receptor fluorescence signals are shown in green (left panels) and specific compartments of the same cells in red (central panels). Cy3 and Alexa Fluor® 488 fluorescence signals were computer-overlaid (right panels; overlap is indicated by yellow). The scans show representative cells. Scale bar, 10 µm. Similar data were obtained in five independent experiments.

The main retention compartment described for mutant V226E is the ERGIC. The verification of ERGIC mutants was done by an incubation of the cells with 1 x 10^{-6} M bafilomycin A1 prior to the immobilization step. Bafilomycin A1 inhibits the retrograde transport of vesicles from the ERGIC to the ER leading to an accumulation of proteins in this particular compartment. This treatment also concentrates the ERGIC-marker protein ERGIC-53, which normally cycles between ER and ERGIC, in this region. After bafilomycin A1 treatment, mutant V226E partially accumulated in structures near the nucleus; ERGIC-53 agglomerated in similar structures. Mutant V226E co-localized with ERGIC-53 indicating an ERGIC localization, but also revealed partial expression in other intracellular structures, presumably the ER. Thus, the quality control system retains mutant V226E in the ER and ERGIC.

The Golgi-marker was a GM130 antibody that recognizes the Golgi-localized protein GM130. Mutant G201D showed a nearly complete overlay with this Golgi-marker (Fig. 6, *lower panel*), but was also located in other intracellular structures.

The present results show that mutant V2Rs are recognized and retained by the cellular quality control system in different intracellular compartments, namely the ER, ERGIC and Golgi apparatus. All intracellular retention compartments ascribed by others could be confirmed with the FLAG-tagged receptor constructs demonstrating that this tag is suitable for studying the degradation pathways of the V2R.

The glycosylation pattern of the mutants was also analyzed to investigate intracellular trafficking. Modification with complex sugar moieties is indicative of transit through the Golgi apparatus. Mutants that fail to acquire complex oligosaccharides are thus retained in pre-Golgi compartments. The stably expressing cell lines were grown to confluence and the FLAG-tagged V2Rs were immunoprecipitated with anti-FLAG affinity gel. The samples were split into three equal aliquots: part one was left untreated (Fig. 7, *C*), whereas the others were digested with Endo H (Fig. 7, *E*) and PNGase F (Fig. 7, *P*), respectively. The samples were subjected to SDS-PAGE and receptors were detected by an anti-FLAG antibody (Fig. 7). The control experiments were performed with untransfected HEK293 cells. Mutant G201D showed a similar pattern to the wild-type receptor (compare 5.1.1): a weak core-glycosylated band at 38 kDa (*) and a prominent mature, complex-glycosylated band at 45 – 55 kDa (♣) (Fig. 7, *upper panel*, *C*). Endo H treatment led to a shift from the core-glycosylated (*) to the non-glycosylated receptor form (#), confirming its localization in pre-Golgi compartments (Fig. 7, *upper panel*, *E*). Digestion with PNGase F revealed a shift of the prominent, complex-gycosylated band (♣) and indicated that most of the mutant receptors were able to reach the Golgi apparatus. As described in 5.1.1, the lack of shift from the complex-glycosylated receptors to the non-glycosylated receptor form is due to additional O-glycosylations (♦). Mutants L62P, V226E and S167L were expressed as immature forms in a 38 kDa band (*), exclusively (Fig. 7, *lower panel, C*). Both enzymes removed the sugar modifications com-

pletely; this could be demonstrated by the detection of sole non-glycosylated receptor forms (#) (Fig. 7, *lower panel, E and P*).

Taken together, the core-glycosylated mutants L62P and V226E are retained in pre-Golgi compartments, whereas the complex-glycosylated mutant G201D reaches the Golgi network and maybe compartments beyond. These findings demonstrate that some mutant receptors are able to escape the quality control of the ER and ERGIC, reach the Golgi apparatus and can be localized in this compartment. Therefore, components of the Golgi apparatus inhibit cell surface expression of mutant receptors and contribute to the quality control system.

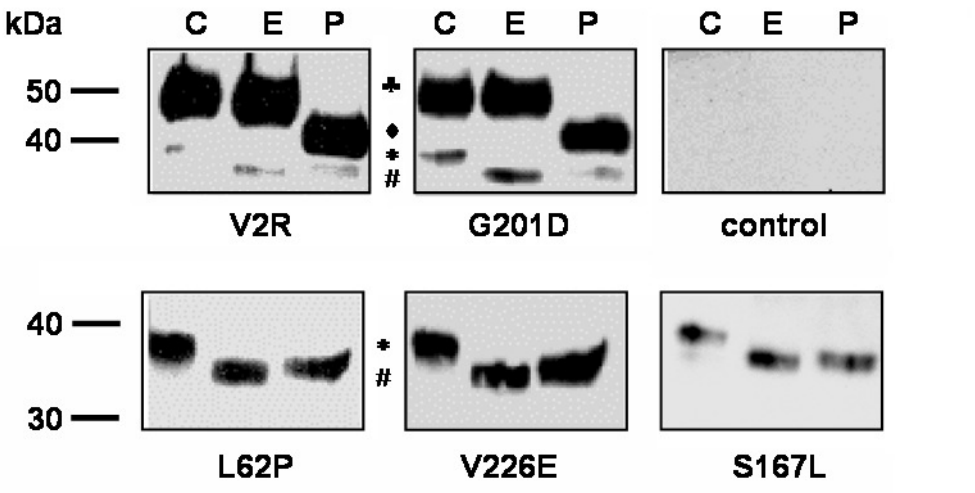

Fig. 7: Endo H and PNGase F digestion of immunoprecipitated fractions of stably expressing HEK293 cells. Cells expressing the FLAG-tagged wild-type V2R and receptor mutants L62P, V226E, S167L and G201D were lysed, immunoprecipitated and digested as indicated in experimental procedures. The samples were analyzed by SDS-PAGE and immunoblotting. Receptor proteins were detected using a monoclonal mouse anti-FLAG antibody and a POD-conjugated goat α-mouse IgG. Immunoreactive bands were developed by ECL. Untreated control samples are shown left (C), Endo H, and PNGase F digested samples in the middle (E) and on the right (P), respectively. The control experiment was performed with untransfected HEK293 cells. The results are representative of three individual experiments.

5.1.7 Adenylyl cyclase activity of mutant receptors

To gain more insight into functional data, the ability of the mutants to activate the adenylyl cyclase system was investigated (Fig. 8). This assay is a sensitive method to characterize the disease-causing mutants of the V2R because it measures the coupling efficiencies of receptors to their signaling pathway. Forskolin was used to adjust the maximum activation of adenylyl cyclases to 100 % and the enzyme activity in the diagram is depicted by black bars (pmol / mg protein / min). The white bars represent the basal activation of adenylyl cyclases in whole membrane fractions without V2R stimulation. Incubation with 100 nM AVP led to a prominent activation of adenylyl cyclases mediated by the wild-type V2R (compare Fig. 3), according to this result the assay was performed with this particular hormone concentration. The basal cAMP levels were at 6 %.

The wild-type V2R showed an adenylyl cyclase activity of 85 % (Fig. 8, *black bar*). Only mutant G201D was able to induce a cAMP response of 50 % indicating that the mutant is functional. As expected, the L62P and the V226E mutants were not able to activate adenylyl cyclases.

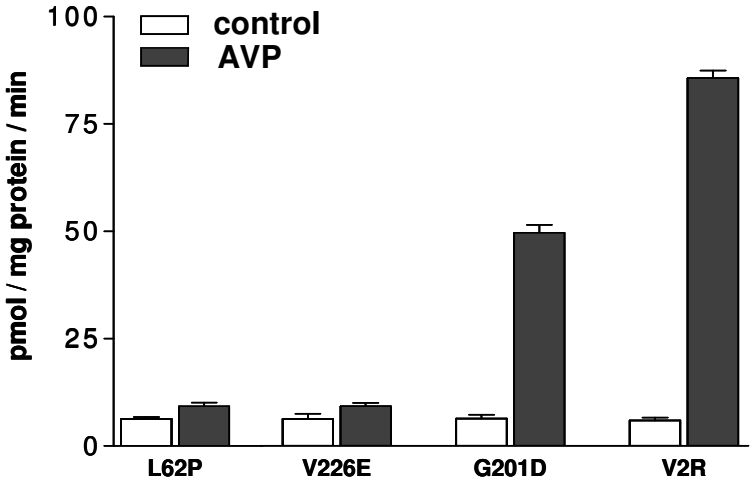

Fig. 8: Adenylyl cyclase activity assay of FLAG-tagged wild-type and mutant V2Rs. Crude membranes of stably transfected HEK293 expressing wild-type and mutant V2Rs were stimulated with 100 nM AVP; controls were performed in the absence of AVP. Data represent mean values of three independent experiments each performed in triplicate. Triplicates differing by less than 10 %. SEM are depicted.

In summary, it could be demonstrated that an N-terminal FLAG-tag does not impair intracellular localization, hormone binding or signaling properties of the V2R and several disease-causing mutants. In addition, the FLAG-tagged V2Rs can be specifically detected in immunofluorescence studies and western blot analysis with high purity. Therefore, the FLAG.V2R fusion proteins provide a suitable tool to study the wild-type receptor and to address the role of the fate of intracellular retained NDI-causing receptor mutants.

5.2 Degradation pathways of V2Rs

In general, cells have two ways to deal with terminally misfolded proteins such as intracellularly retained V2R mutants to reduce cell stress. Some misfolded proteins may accumulate in the cytoplasm and are deposited in inclusion bodies or aggresomes (Waelter, Boeddrich et al. 2001). Formation of these protein aggregations often leads to apoptosis. Other non-native proteins may activate the unfolded protein response (UPR) pathway, a series of answers to high amounts of ER-residing misfolded proteins. Chaperones and enzymes that assist in protein folding are up-regulated under UPR conditions and terminally misfolded proteins are subjected to ERAD. Until now, the precise mechanism by which proteins retained in compartments beyond the ER are recognized and degraded remains to be elucidated.

Microscopic analysis does not reveal any accumulations of the GFP-tagged mutant L62P in inclusion bodies or aggresomes in the cytoplasm with or without blocking of proteasomal turnover (Fig. 9), but the intensity of the fluorescence signals was increased in cells treated with the proteasome inhibitor MG132. The survival of cell lines stably expressing mutant V2Rs also contributes to the assumption that at least some cells are able to adapt to stress caused by intracellular retained proteins. These findings strongly support the conclusion that the intracellular retained mutant receptors are efficiently degraded.

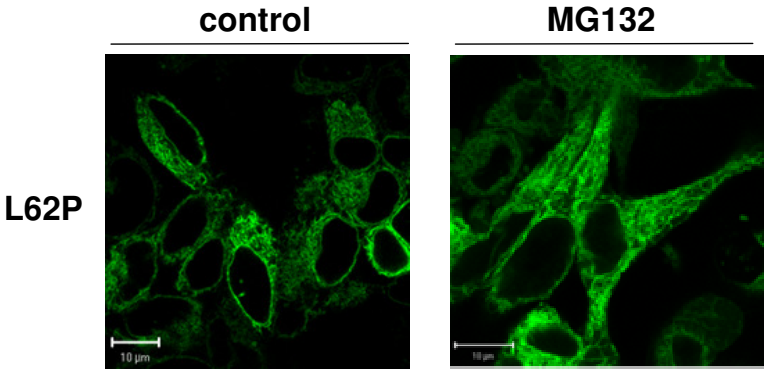

Fig. 9: Microscopic analysis of living HEK293 cells stably expressing the ER-retained GFP-tagged V2R mutant L62P. Cells were grown for 24 h and were incubated without or with 20 µM MG132 for 16 h. Receptor GFP fluorescence signals are shown in green. The scans show representative cells. Scale bar, 10 µm. Similar data were obtained in three independent experiments.

5.2.1 Pulse-chase analysis reveals insight in degradation pathways of wild-type and intracellular retained V2Rs

Two main pathways that facilitate protein turnover operate in cells. Lysosomes commonly degrade long-lived proteins residing at the plasma membrane, proteins ingested

by endocytosis or large cytoplasmic organelles. The ubiquitin / proteasome system is responsible for destruction of short-lived, intracellular proteins; it mediates many specific cellular regulation processes including degradation of misfolded proteins. To investigate the degradation pathway of V2Rs, pulse-chase experiments were performed in presence or absence of inhibitors of both pathways. The lysosomal degradation was impeded with chloroquine, an inhibitor of lysosomal hydrolases. MG132 blocked proteasomal turnover; the substance is a reversible inhibitor of the trypsin- and chymotrypsin-like activities of the catalytic core of the 26S proteasome.

Cells were starved overnight in medium without the amino acids methionine and cysteine, so that overall protein synthesis was halted. Cells were radiolabeled with Easy-Tag™ EXPRESS^{35}S Protein Labeling Mix for 45 min, the protein synthesis initiated again and radiolabeled methionine and cysteine were incorporated. The reaction was stopped with an excess of unlabeled amino acids and after indicated times (0, 2.5, 5, 10 h) cells were harvested, lysed and the V2Rs were immunoprecipitated. After separation by SDS-PAGE, gels were dried on a gel dryer and receptors were visualized by autoradiography.

The pulse-chase assay was performed under control conditions (untreated) and under inhibition of lysosomal enzymes (chloroquine) or proteasomal activity (MG132) (Fig. 10). The wild-type V2R was expressed in two receptor forms directly after the end of the labeling process (0 h) (Fig. 10, *left panel, top*). The first 35 kDa band corresponds to the non-glycosylated receptors and the second 38 kDa band to the core-glycosylated receptor form. After 2.5 h the complex-glycosylated receptors appear at 45 – 55 kDa and both immature forms were less prominent. After 5 h the non-glycosylated receptors were not detectable. The mature receptors were not completely degraded within 10 h, which indicates that they have a longer biological half-life than 10 h. A small amount of core-glycosylated receptors was still detectable after 10 h. Inhibition with chloroquine (*middle panel*) did not show an effect on the stability of the complex-glycosylated form, or on the immature forms of the V2R. Proteasomal degradation was inhibited with MG132 (*right panel*) and led to an increase in the stability of non- and core-glycosylated receptor forms, whereas the complex-glycosylated form was unaffected. Thus, immature V2R forms are mainly degraded in proteasomes. G201D, the Golgi-localized mutant, showed a similar degradation pattern as the V2R (Fig. 10, *middle panels, untreated*). In contrast to the wild-type receptor, the chloroquine-induced inhibition caused an increase in the intensity of the complex-glycosylated receptor form, indicating a lysosomal degradation pathway for the mature receptor mutant. Proteasomal inhibition additionally stabilized the immature receptor forms, showing that G201D is degraded by both pathways.

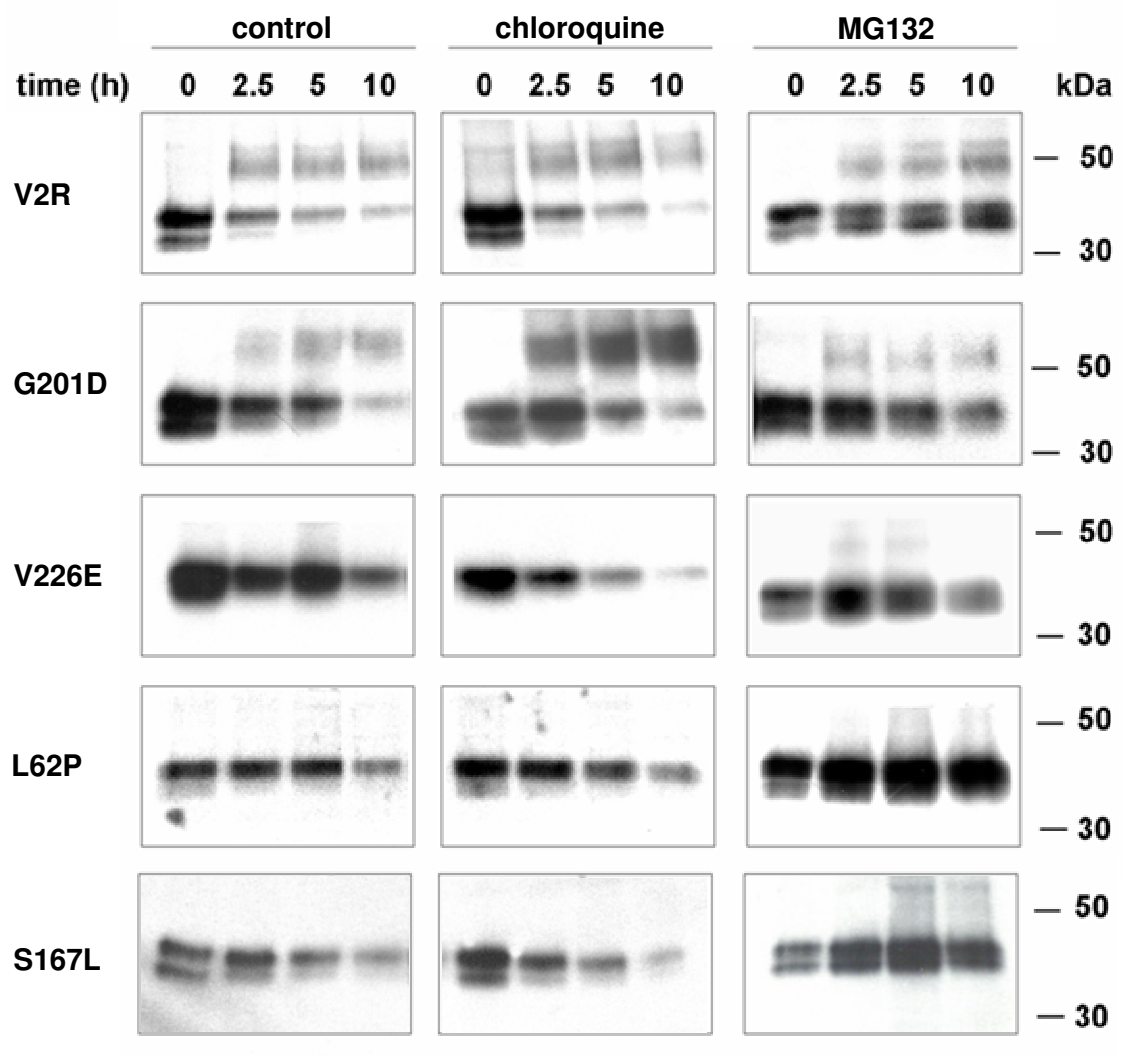

Fig. 10: Degradation of wild-type V2R and NDI-causing mutants in stably expressing HEK293 cells. Cells expressing the FLAG-tagged wild-type V2R and receptor mutants L62P, S167L, V226E and G201D were starved in serum-free DMEM without methionine and cysteine for 16 h and metabolically labeled with 220 µCi [^{35}S] EasyTag EXPRESS^{35}S Protein Labeling Mix for 45 min without (*left panel*) or in presence of 100 µM chloroquine (*center*) or 40 µM MG132 (*right panel*). The metabolic labeling was stopped and at time points 0, 2.5, 5, and 10 h the cells were harvested, lysed and immunoprecipitated as described in "Methods" and proteins were separated by SDS-PAGE. The gels were dried and exposed to X-ray films. Molecular mass markers are shown on the right. The results are representative of three individual experiments.

The ERGIC-located mutant V226E and the ER-retained mutants L62P and S167L were expressed as immature forms; they only showed two bands in agreement with previous data described in this work. The degradation half-life of their core-glycosylated form was extended in comparison to the degradation half-life of core-glycosylated forms of wild-type V2R and mutant G201D, maybe due to the lack of transport to the Golgi apparatus. Chloroquine had no apparent effect on the degradation process, whereas MG132 stabilized all immature forms indicating proteasomal turnover of non- and core-glycosylated mutant V2Rs. To exclude that the stabilization of immature receptors was

an effect of the proteasome inhibitor MG132, a second, irreversible proteasome inhibitor, lactacystin, was used to test the degradation of the wild type V2R. This substance also caused stabilization of both immature receptor forms (data in appendix, App. Figure 1) indicating that the lack of breakdown was not due to the influence of MG132.

Taken together, all immature receptor forms of wild-type and mutant receptors are sensitive to proteasome inhibitors which supports the idea that they are substrates for the ER-associated degradation pathway culminating in proteasomal turnover. Lysosomal inhibition only seems to play a role for the stabilization of the complex-glycosylated form of mutant G201D. Therefore, lysosomes contribute to intracellular quality control.

5.2.2 Lysosomal localization determined in living cells

To investigate the participation of the lysosomal degradation pathway, especially on mutant G201D, the V2R constructs were analyzed for co-localization with lysosomal dyes using confocal laser-scanning microscopy. For visualization of the receptors, HEK293 cell lines stably expressing C-terminal GFP-tagged receptor proteins (Fig. 11, 12, 13, 14; *green channel*) were transferred into a heating chamber at 37 °C. Lysosomal vesicles were stained with 150 nM LysoTracker Red for 1 h (Fig. 11, 12, 13, 14; *red channel*) and overlays of both channels were computed.

Mutant L62P showed a diffuse intracellular distribution excluding the nuclear region. Lysosomes were found as vesicular structures in the cytoplasm, frequently nearby the nucleus. No co-localization could be observed between mutant L62P and lysosomes (Fig. 11, *overlay*); lysosomal vesicles were located in the same area as the receptors, but for a real co-localization similar structures have to be present. Treatment with chloroquine did not affect the localization of mutant L62P (Fig. 11, *overlay*). Mutant V226E showed neither co-localization with lysosomes in control cells (Fig. 11, *overlay*), nor in chloroquine-treated cells (Fig. 12, *overlay*). The complex-glycosylated mutant G201D was found at the plasma membrane and also appeared to be partially localized in endocytic vesicles. The overlay between lysosomes and mutant G201D yielded a partial co-localization (Fig. 11, *overlay*). Incubation with the lysosomal inhibitor chloroquine led to a strong increase of two intracellular signals: 1) the number of receptors located in vesicles and 2) the number of lysosomal vesicles, which were clustered in an area close to the nucleus (Fig. 12, *overlay*). The same was observed for the wild-type V2R, which was mainly expressed at the plasma membrane, but was also apparent in intracellular structures co-localizing with LysoTracker Red signals (Fig. 11 and 12, *overlay*).

The complex-glycosylated V2Rs, wild-type and mutant G201D, are transported to the lysosomal compartment for degradation at steady state. The core-glycosylated mutants L62P and V226E are retained by the quality control in ER and ERGIC and are excluded

from lysosomal turnover. Thus, the ERGIC seems to be the last compartment in the secretory pathway that excludes membrane proteins from lysosomal degradation.

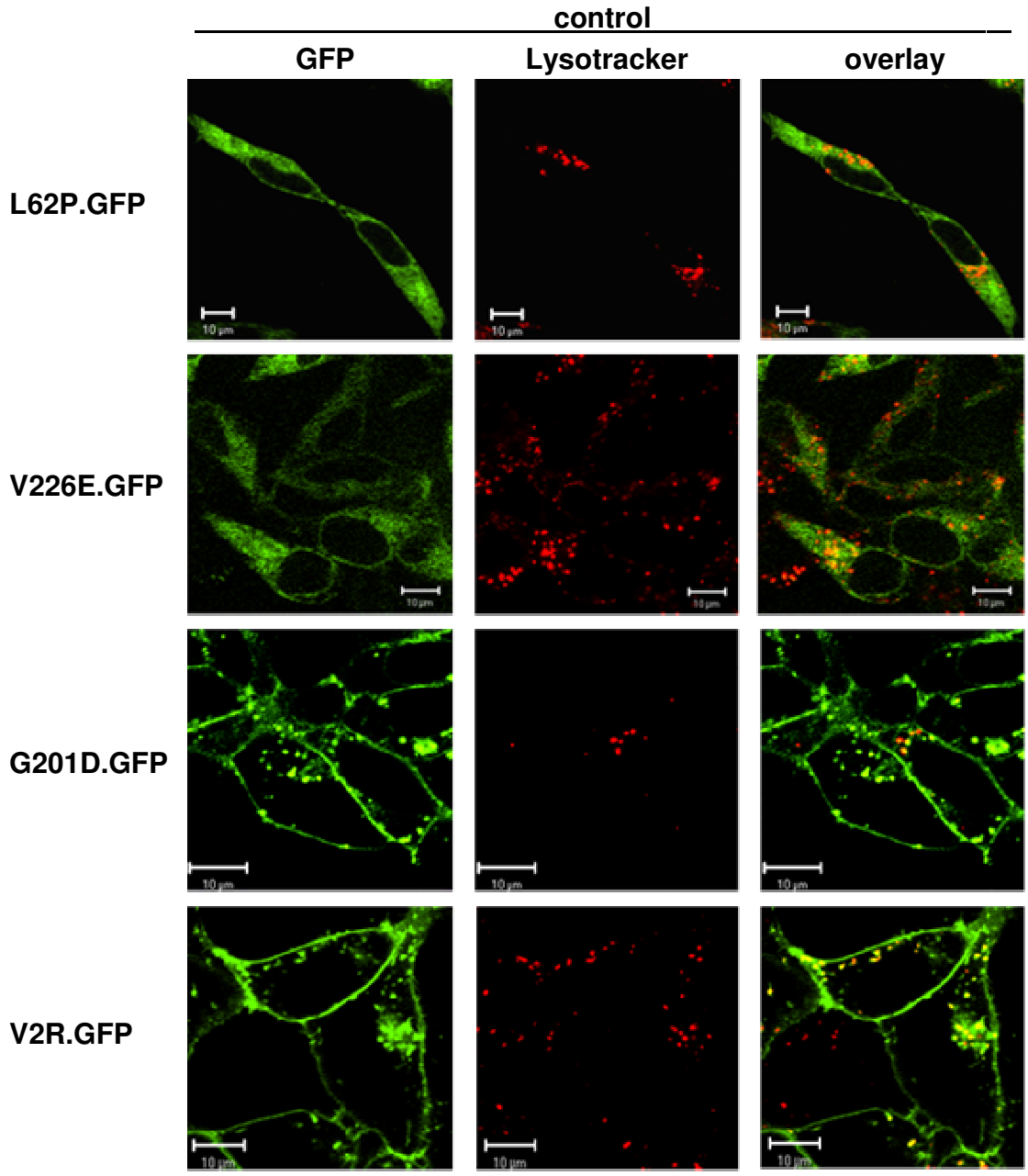

Fig. 11: Lysosomal localization of GFP-tagged wild-type V2R and mutants L62P, V226E, and G201D analyzed in stably expressing, living HEK293 cells. Cells were incubated with 150 nM LysoTracker Red for 1 h and were examined by confocal laser scanning microscopy with horizontal (xy) scans. Receptor GFP fluorescence signals are shown in green (left panels) and LysoTracker Red staining of the same cells in red (central panels). GFP and Lyso-Tracker Red fluorescence signals were computer-overlaid (right panels; overlap is indicated by yellow). The scans show representative cells. Scale bar, 10 µm. Similar data were obtained in five independent experiments.

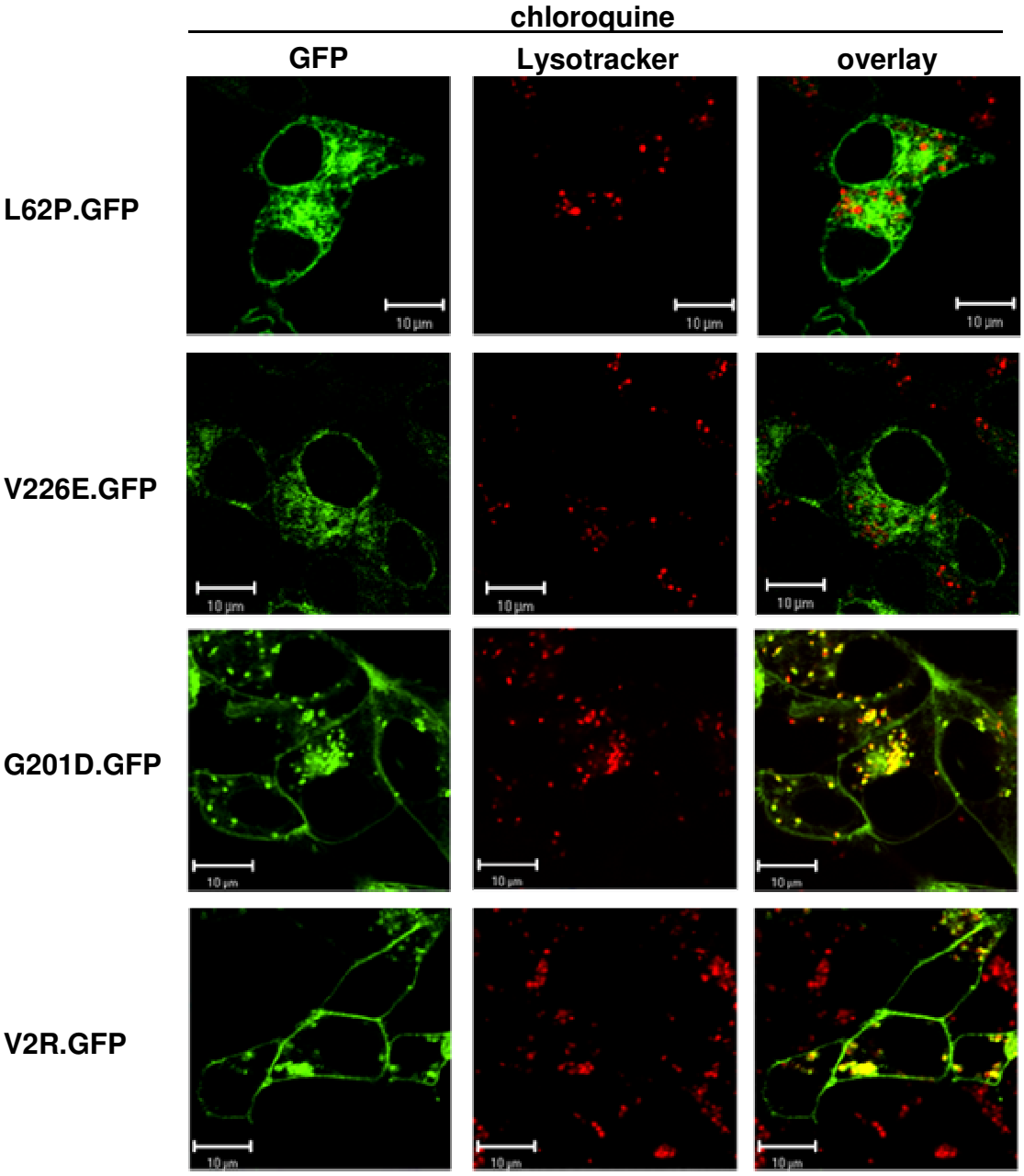

Fig. 12: Inhibition of lysosomal degradation analyzed in living HEK293 cells stably expressing the GFP-tagged wild-type V2R and mutants L62P, V226E, and G201D. Cells were incubated in presence of 100 µM chloroquine for 3 h and 150 nM LysoTracker Red for 1 h and were examined by confocal laser scanning microscopy with horizontal (*xy*) scans. Receptor GFP fluorescence signals are shown in green (left panels) and LysoTracker Red staining of the same cells in red (central panels). GFP and LysoTracker Red fluorescence signals were computer-overlaid (right panels; overlap is indicated by yellow). The scans show representative cells. Scale bar, 10 µm. Similar data were obtained in five independent experiments.

For further analysis of the degradation pathways, the stabilization of all immature receptor forms in presence of MG132 obtained in the pulse-chase experiments was taken into account. In living HEK293 cells stably expressing wild-type and mutant receptors the proteasome inhibitor MG132 had no influence on receptor localization or lysosomal localization (Fig. 13 & 14).

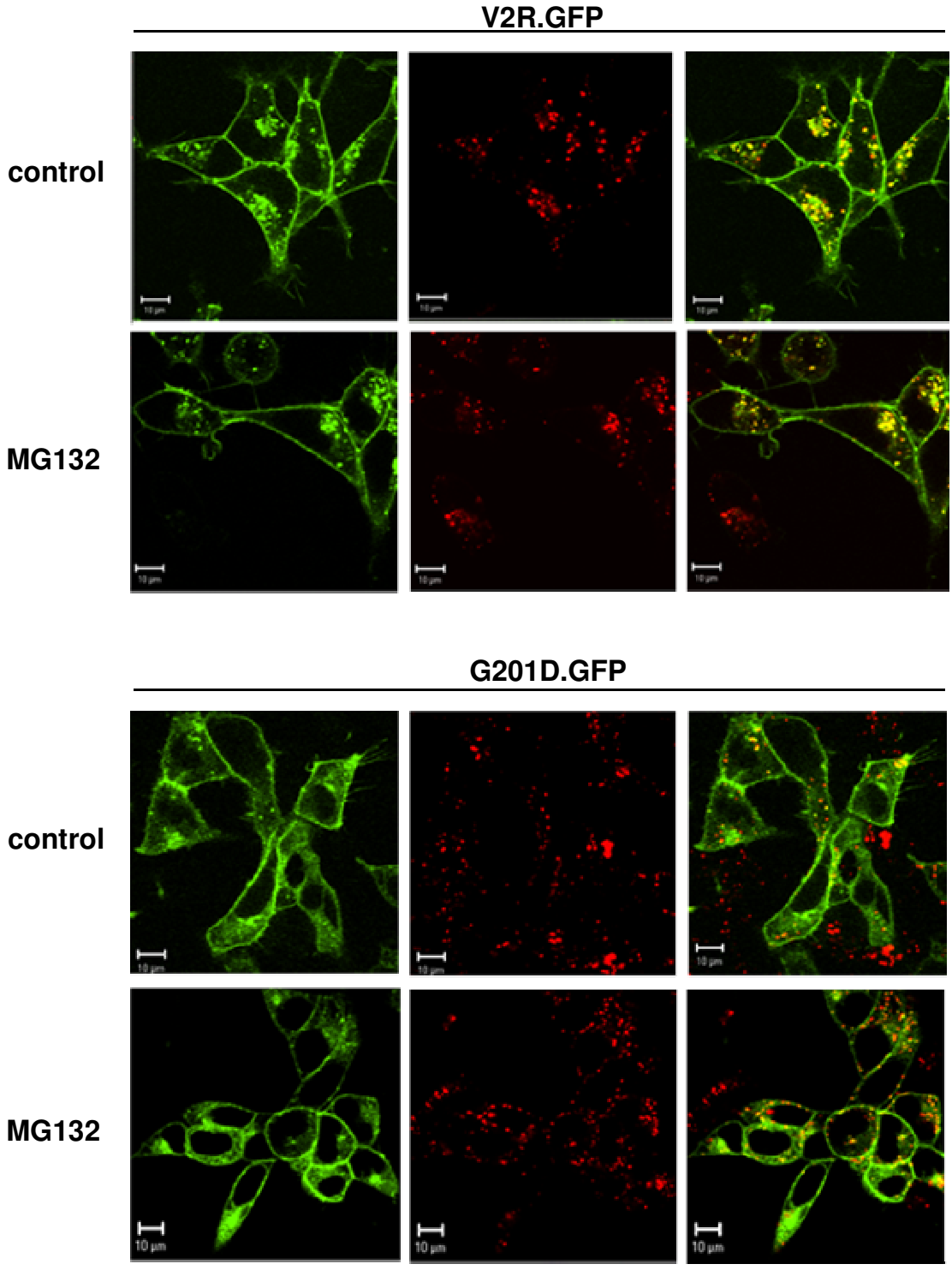

Fig. 13: Inhibition of proteasomal degradation analyzed in living HEK293 cells stably expressing the GFP-tagged wild-type V2R and mutant G201D. Cells were incubated in presence of 40 µM MG132 for 4 h and 150 nM LysoTracker Red for 1 h and were examined by confocal laser-scanning microscopy with horizontal (*xy*) scans. Receptor GFP fluorescence signals are shown in green (left panels) and LysoTracker Red staining of the same cells in red (central panels). GFP and LysoTracker Red fluorescence signals were computer-overlaid (right panels; overlap is indicated by yellow). The scans show representative cells. Scale bar, 10 µm. Similar data were obtained in three independent experiments.

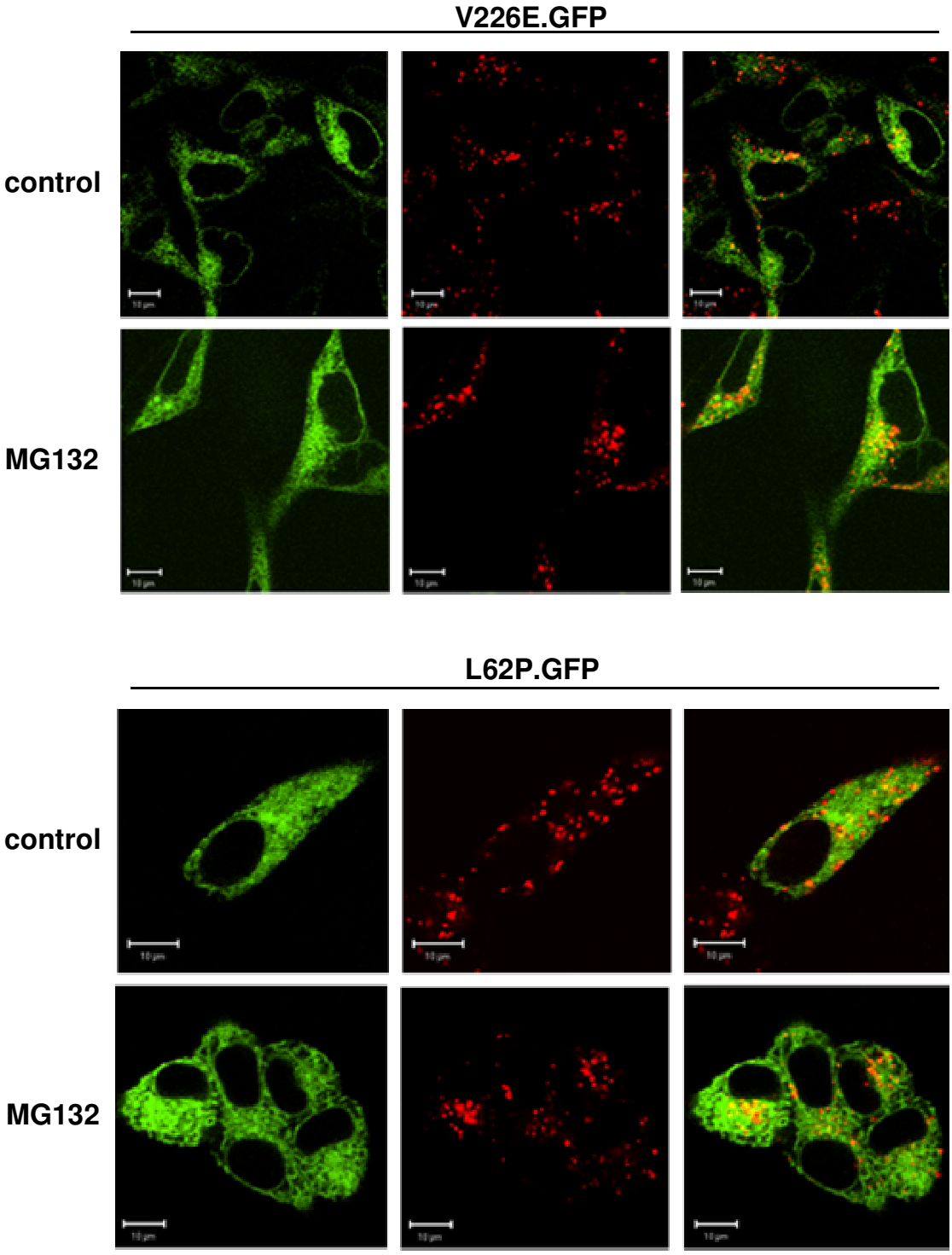

Fig. 14: Inhibition of proteasomal degradation analyzed in living HEK293 cells stably expressing the GFP-tagged V2R mutants L62P and V226E. Cells were incubated in presence of 40 µM MG132 for 4 h and 150 nM LysoTracker Red for 1 h and were examined by confocal laser-scanning microscopy with horizontal (*xy*) scans. Receptor GFP fluorescence signals are shown in green (left panels) and LysoTracker Red staining of the same cells in red (central panels). GFP and LysoTracker Red fluorescence signals were computer-overlaid (right panels; overlap is indicated by yellow). The scans show representative cells. Scale bar, 10 µm. Similar data were obtained in three independent experiments.

5.2.3 Ubiquitination and proteasomal degradation

Polyubiquitination is a prerequisite for recognition and degradation of a multiplicity of substrate proteins by the 26S proteasome (Ciechanover 2005); only a few substrates are degraded without this post-translational modification (Hoyt and Coffino 2004; Asher and Shaul 2005). Specific ubiquitin ligases transfer the polyubiquitin-chains on lysine or cysteine residues of target proteins (Kostova, Tsai et al. 2007). First, the receptor's polyubiquitination status was investigated.

For this, HEK293 cell lines stably expressing FLAG-tagged wild-type V2R and mutant receptors were treated with MG132 to block proteasomal turnover and to accumulate ubiquitinated and non-ubiquitinated proteins. Cells were subsequently lysed and receptors were immunoprecipitated by the FLAG-epitope and analyzed by SDS-PAGE and Western Blot. The ubiquitinated V2Rs were detected by an anti-multiubiquitin antibody (Fig. 15, *A*). Control cells were untransfected HEK293 cells and, despite MG132 treatment, no ubiquitin signal was apparent. The control sample only showed two unspecific bands and one band running at 60 kDa that corresponds to the heavy chain of the precipitating antibody. In untreated wild-type expressing cells a weak smear of ubiquitinated receptors was detected starting at 250 kDa. The intensity of this smear was strongly enhanced in MG132-treated cells (60 - 250 kDa). This smear is typical for ubiquitinated proteins, since ubiquitin chains of different lengths are coupled by E3 enzymes. All tested receptors, mutants and wild-type V2R, showed modifications corresponding to polyubiquitin.

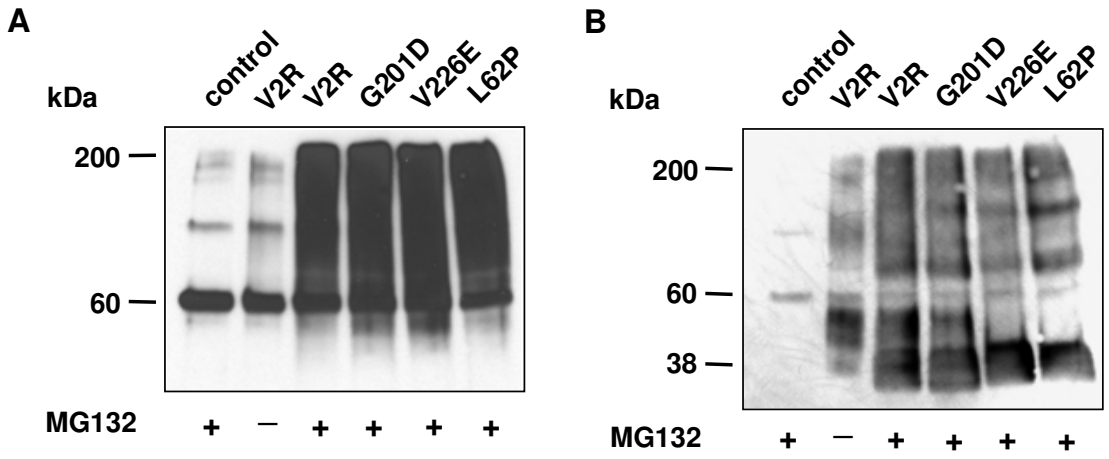

Fig. 15: Ubiquitination of FLAG-tagged V2Rs. *A*, immunoprecipitation of polyubiquitinated receptors. HEK293 cells stably expressing wild-type and mutant V2Rs were treated with 20 µM MG132 for 16 h or left untreated. Proteins eluted from anti-FLAG affinity gel were analyzed by SDS-PAGE and western blot analysis with a monoclonal mouse α-polyubiquitin antibody and a POD-conjugated α-mouse antibody. *B*, stably expressing HEK293 cells were lysed and receptors were immunoprecipitated as in *A* and detected with a polyclonal α-FLAG antibody, a POD-conjugated α-rabbit antibody and the ECL system. Data are representative of four independent experiments.

In a second approach, the experiment was repeated, but this time the receptors were detected by an anti-FLAG antibody to demonstrate equal protein precipitation between the samples (Fig. 15, *B*). As expected, the control cells only revealed unspecific immunoreactive bands. The immunoblot showed high-molecular receptor forms of 60 – 250 kDa in a similar smear detected in the ubiquitin blot. The sample of untreated cells expressing the V2R showed the mature 45 – 55 kDa form and was devoid of the non-glycosylated form. In the MG132 treated wild-type receptor and mutant G201D samples, detected receptor proteins were expressed as non-, core-, and complex-glycosylated forms (35, 38, 50 kDa), whereas V226E and L62P only showed non- and core-glycosylated receptor forms (35, 38 kDa). All HEK293 cell lines expressed the receptor constructs in comparable amounts. To verify the results concerning the ubiquitination state, a second, reverse immunoprecipitation was performed.

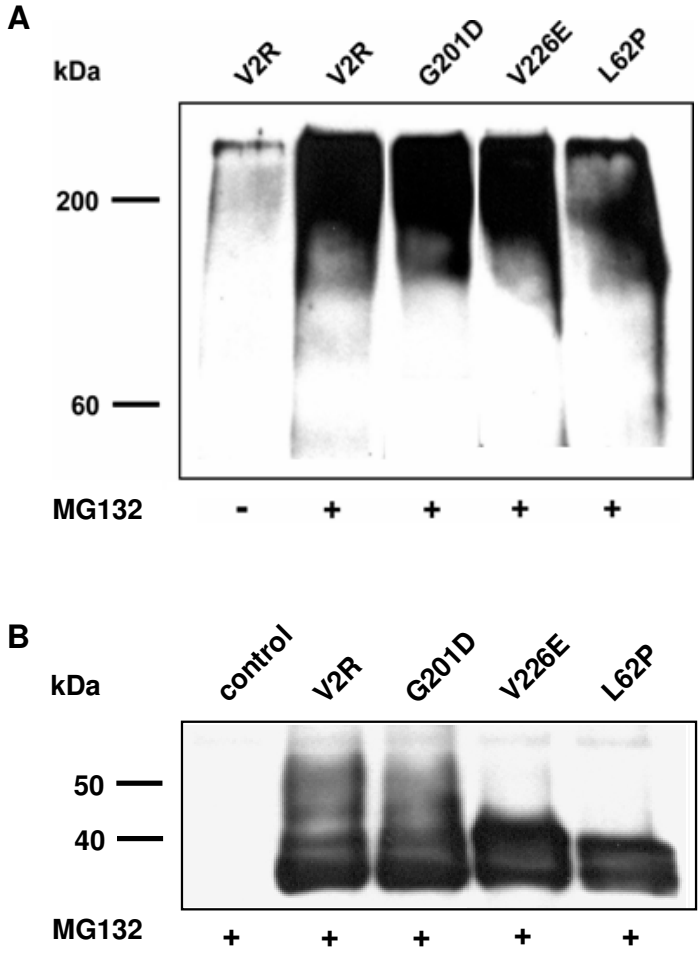

Fig. 16: Immunoprecipitation of ubiquitinated wild-type and mutant V2Rs. The stably expressing HEK293 cells (V2R wild-type and mutant receptors) were treated with 20 µM MG132 for 16 h or left untreated. *A*, immunoprecipitation of polyubiquitinated proteins with polyubiquitin enrichment beads. Proteins eluted from the beads were analyzed for the V2Rs by western blotting with the α-FLAG antibody and a POD-conjugated anti-mouse antibody. This blot is representative of similar blots from four independent experiments. *B*, immunoprecipitation of receptors with an immune-complex of anti-FLAG antibodies and protein A-Sepharose. Proteins were separated by SDS-PAGE and subsequently analyzed by western blotting. Receptors were detected by a rabbit anti-FLAG antibody, a POD-coupled secondary antibody and the ECL system. Controls were untransfected HEK293 cells. This blot is representative of three individual experiments.

Lysates containing FLAG-tagged receptors were subjected to immunoprecipitation with polyubiquitin enrichment beads that precipitate all cellular polyubiquitinated proteins. Subsequently, the precipitated proteins were analyzed by SDS-PAGE and western blot. For receptor detection antibodies against the FLAG-epitope were used (Fig. 16, *A*). A prominent immunoreactive smear was detectable between 80 and 250 kDa in all analyzed samples pre-incubated with the proteasome inhibitor MG132. Unfortunately, detection of receptors on the same nitrocellulose membrane was not possible. The controls of receptor expression were therefore precipitated in a parallel experiment with anti-FLAG affinity gel and detected by an anti-FLAG antibody (Fig 16, *B*). The immunoprecipitation of the different V2Rs revealed comparable receptor levels between the utilized cell lines. The assay confirmed the previous result that all receptors, wild-type V2R and all tested mutants, are polyubiquitinylated prior to degradation and are suitable substrates for ERAD.

To exclude the possibility that the lysines of the N-terminal FLAG-tag were responsible for ubiquitination, the FLAG-tag was exchanged for a lysine-free haemagglutamin (HA)-tag. The HA.V2R cDNA was transiently transfected in HEK293 cells and immunoprecipitated with covalent coupled HA-beads. After SDS-PAGE and western blot, samples were analyzed for expression, glycosylation pattern (Fig. 17, *A*) and ubiquitination state (Fig. 17, *B*). HA-tagged receptors were expressed in the common bands of 38 kDa and 45 – 55 kDa. The HA-tagged receptors were polyubiquitinated indicated by an ubiquitin smear of 60 – 250 kDa (Fig. 17, *B*, *upper panel*), confirming that the lysine-containing FLAG-tag is not responsible for false positive results.

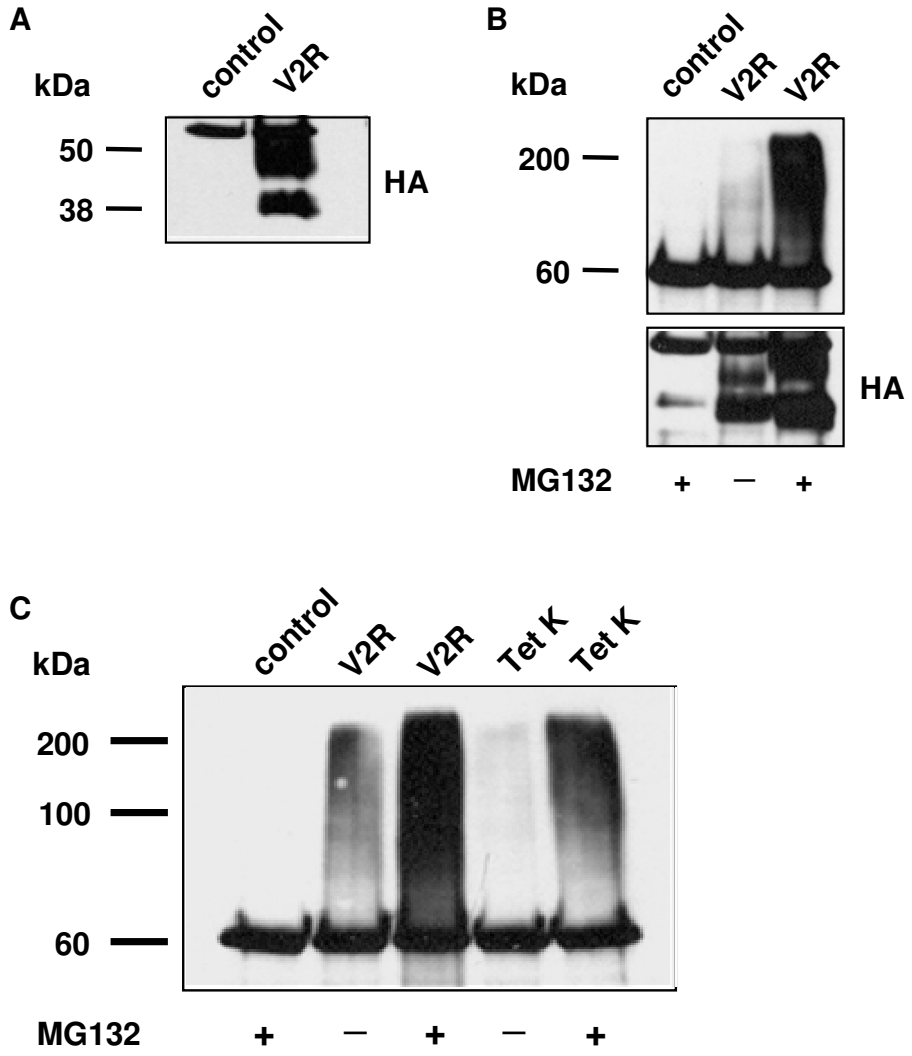

Fig. 17: Ubiquitination status of HA-tagged V2Rs transiently expressed in HEK293 cells. *A*, HEK293 cells were transiently transfected with HA.V2R cDNA and were grown for 48 h. Cells were lysed and the receptors were immunoprecipitated by anti-HA beads. Proteins eluted from the beads were analyzed for the V2Rs by western blotting with an anti-HA antibody and a POD-conjugated secondary antibody. This blot is representative for three independent experiments. *B*, immunoprecipitation of receptors with anti-HA beads. Proteins were separated by SDS-PAGE and subsequently analyzed by western blotting. Ubiquitinated receptors were detected by a mouse anti-multiubiquitin antibody, a POD-coupled secondary antibody and the ECL system (*upper panel*). Controls were untransfected HEK293 cells. After stripping of the membrane, receptor proteins were detected by anti-HA antibodies (*lower panel*). These blots are representative of three individual experiments. *C*, western blot analysis and detection of ubiquitinated wild-type and mutant V2Rs was performed as in *B* (upper panel).

Transient transfection led to an increased rate of core-glycosylated receptors (Fig. 17, *B*, *lower panel, middle lane*) compared to the stably FLAG.V2R expressing cell lines (compare Fig.1, *V2R*, *C*). The same phenomenon had been observed for transiently transfected FLAG-tagged receptors and was one reason for the generation of the stably expressing cell lines (data not shown). As expected, MG132 treatment stabilized the non- and core-glycosylated receptor form of the HA-tagged V2R (Fig. 17, *B*, *lower panel, right lane*). In an attempt to abrogate the modification of V2Rs with ubiquitin, all lysines of the HA-tagged wild-type V2R were substituted with arginine. The K100 / 116

/ 286 / 368R mutant was named Tet K, subjected to immunoprecipitation via the HA-epitope and western blot analysis and was probed for polyubiquitin (Fig. 17, *C*). As expected the HA-tagged wild-type V2R showed an ubiquitin smear from 60 – 250 kDa, which increased in presence of MG132. In addition, proteasome inhibition led to detection of polyubiquitinated lysine-free Tet K, but the ubiquitin signal intensity was more prominent for the wild-type V2R.

The results of the ubiquitination status experiments of the V2R and its disease-causing mutants lead to the hypothesis that the receptor's lysine and / or cysteine residues are polyubiquitinated. But it cannot be reliably excluded that an interacting protein is ubiquitinated as well, which was co-precipitated and co-detected. However, taking into account the previous pulse-chase experiments, a proteasomal degradation pathway of immature V2R forms is a highly possible explanation.

5.2.4 ER-associated degradation (ERAD)

For ER-retained misfolded proteins, the ERAD pathway operates to diminish ER stress and to facilitate substrate degradation by the cytoplasmatic proteasome. Proteins that are recognized by the ERGIC quality control system may be transported back to the ER (Hermosilla, Oueslati et al. 2004). There might also be a retrograde pathway for the transport of Golgi-retained proteins to the ER (Caldwell, Hill et al. 2001). Since pre-Golgi accumulations of immature receptors were induced by proteasome inhibitors, the involvement of the ERAD pathway was hypothesized. To elucidate the role of the ERAD in the degradation of wild-type V2R and its mutants, the interactions of canonical ERAD components with the receptors were investigated. The AAA ATPase p97/VCP is central to all known ERAD pathways and was therefore chosen for the following experiments (Fig. 18 *A* and *B*).

In untreated total cell lysates, equal expression levels of p97/VCP could be demonstrated; all cell lines showed an immunoreactive band at 98 kDa and expressed comparable amounts of p97/VCP (Fig. 18, *A, upper panel*). Treatment with MG132 did not alter the amounts of expressed p97/VCP (data not shown). The expression of actin was used as a loading control (Fig. 18, *A, lower panel*).

HEK293 cell lines stably expressing the FLAG.V2R fusion proteins were treated with MG132 to stop proteasomal degradation, lysed, and the receptors were immunoprecipitated with anti-FLAG affinity gel. After SDS-PAGE and western blot analysis, nitrocellulose membranes were incubated with p97/VCP antibodies to identify co-precipitated proteins (Fig. 18, *B*). The immunoprecipitation study revealed that the wild-type and all tested mutants were able to co-precipitate p97/VCP in a specific immunoreactive band at 98 kDa under the influence of MG132 (Fig. 18, *B, middle panel*).

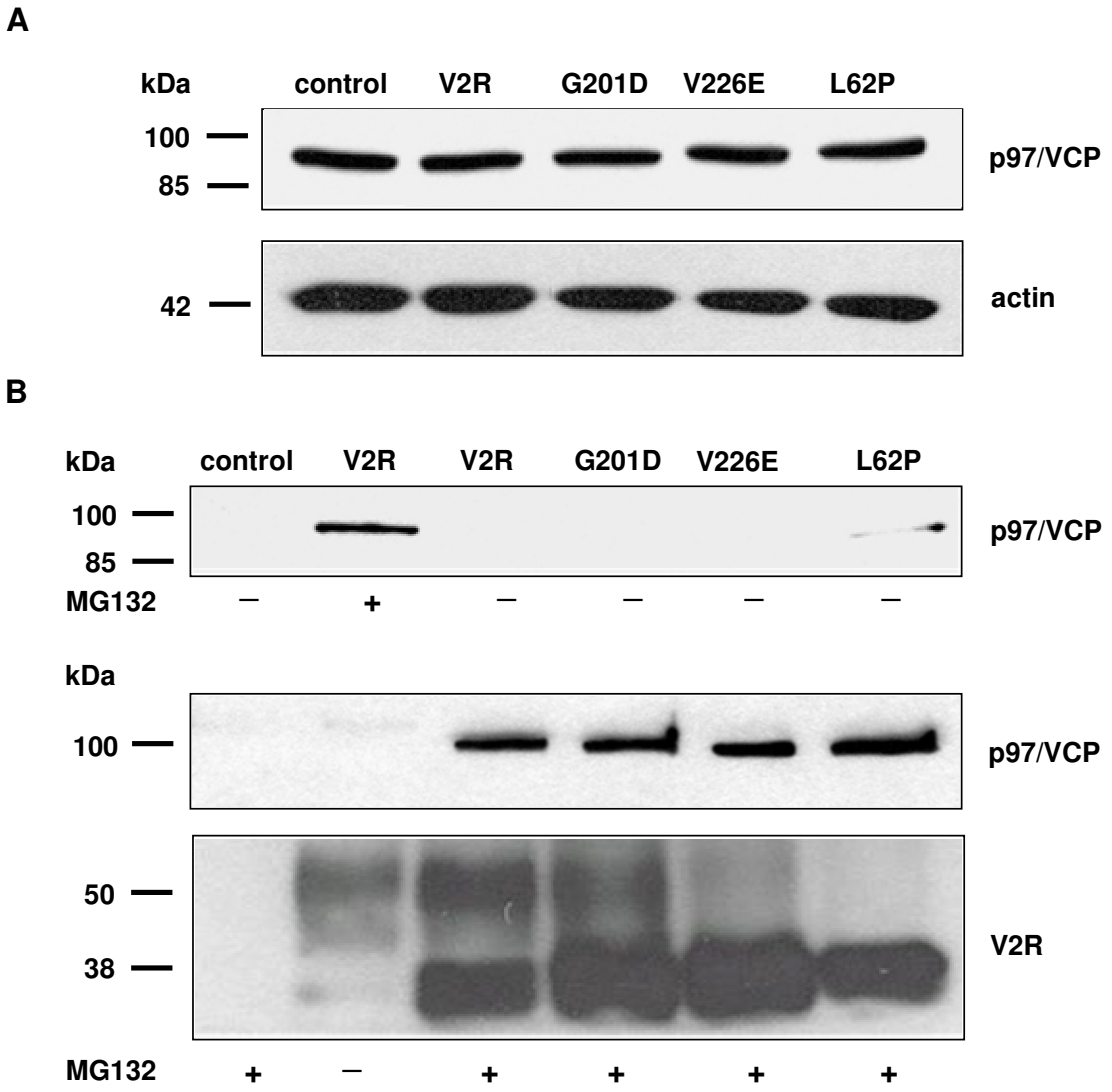

Fig. 18: Interaction of the V2R and NDI-causing mutants with the AAA ATPase p97/VCP. HEK293 cells stably expressing wild-type and mutant V2Rs were treated with 20 µM MG132 for 16 h (+) or left untreated (-). *A*, total cell lysates analyzed by western blotting for p97/VCP expression are shown in the top panel. *B*, receptor proteins were immunoprecipitated and analyzed by western blot in the middle panels. Detection of co-precipitated p97/VCP was done with a polyclonal rabbit α-p97/VCP antibody, POD-conjugated α-rabbit antibody and the ECL system. Receptors were detected by a mouse anti-FLAG antibody (*lower panel*). Controls were non-transfected HEK293 cells. Representative blots of three independent experiments are shown.

Controls were untransfected HEK293 cells and showed no specific signal. The ER retained mutant L62P was also able to precipitate p97/VCP without inhibition of the degradation process (Fig. 18, *B, upper panel*) indicating an interaction of this mutant with p97/VCP at steady state. Equal expression levels of receptor proteins were controlled by stripping of the membranes and subsequent detection of FLAG-tagged proteins (Fig. 18, *B, lower panel*). This assay proves that the ERAD pathway is involved in turnover of immature forms of the wild-type V2R and all tested mutant V2Rs.

5.2.5 Involvement of different ERAD pathways in turnover of V2Rs

Growing evidence is emerging that depending on the substrate protein different ERAD pathways facilitate protein turnover. Recently, Carvalho et al. described three independent ERAD pathways in yeast that degrade dislocation substrates dependent on the localization of the misfolded domain: cytoplasmatic, transmembrane or ER-luminal (Carvalho, Goder et al. 2006). It is not clear if these distinct pathways also operate in mammalian cells. The three ascribed pathways differ in a central ERAD component: the putative translocation channel protein Der1, which is most likely important for ERAD substrates to overcome the ER membrane for cytoplasmic degradation. The ERAD-C pathway eliminates substrates with misfolded cytoplasmic domains independent of Der1. The Doa10 ligase, which is presumed to be the yeast homolog of TEB4, is the key component of the degradation complex. Central to the ERAD-M and ERAD-L pathways that are involved in degradation of substrates with misfolded transmembrane- or luminal regions, respectively, is the ubiquitin ligase Hrd1. The gene encoding Hrd1 is conserved from yeast to humans. Therefore the ERAD-M pathway is proposed to be independent of Der1, whereas it is necessary in the ERAD-L system. All ERAD pathways use the ATPase complex of Ubx2, Cdc48 (yeast counterpart of p97/VCP) and the cofactors Np14 and Ufd1. To elucidate the involvement of distinct mammalian ERAD pathways in the turnover of mutant V2Rs, the presence of Derlin-1 was analyzed in relation to all mutant receptors.

First, the endogenous expression levels of Derlin-1 were analyzed in whole cell lysates (FIG. 19, *A*) and a single band with an apparent size of 22 kDa could be identified in all samples. The same lysates were also controlled by detection of actin, and both images revealed no differences in the expression levels of Derlin-1 and actin between untransfected HEK293 cells (control) and the stably expressing cell clones. For the co-immunoprecipitation study, receptors were pulled down with anti-FLAG affinity gel and separated by SDS-PAGE. Co-precipitated Derlin-1 was identified by an anti-Derlin-1 antibody, which detected a weak, but specific band at 22 kDa in wild-type and mutants expressing cells without the proteasome inhibitor MG132 (Fig. 19, *B, upper panel*).

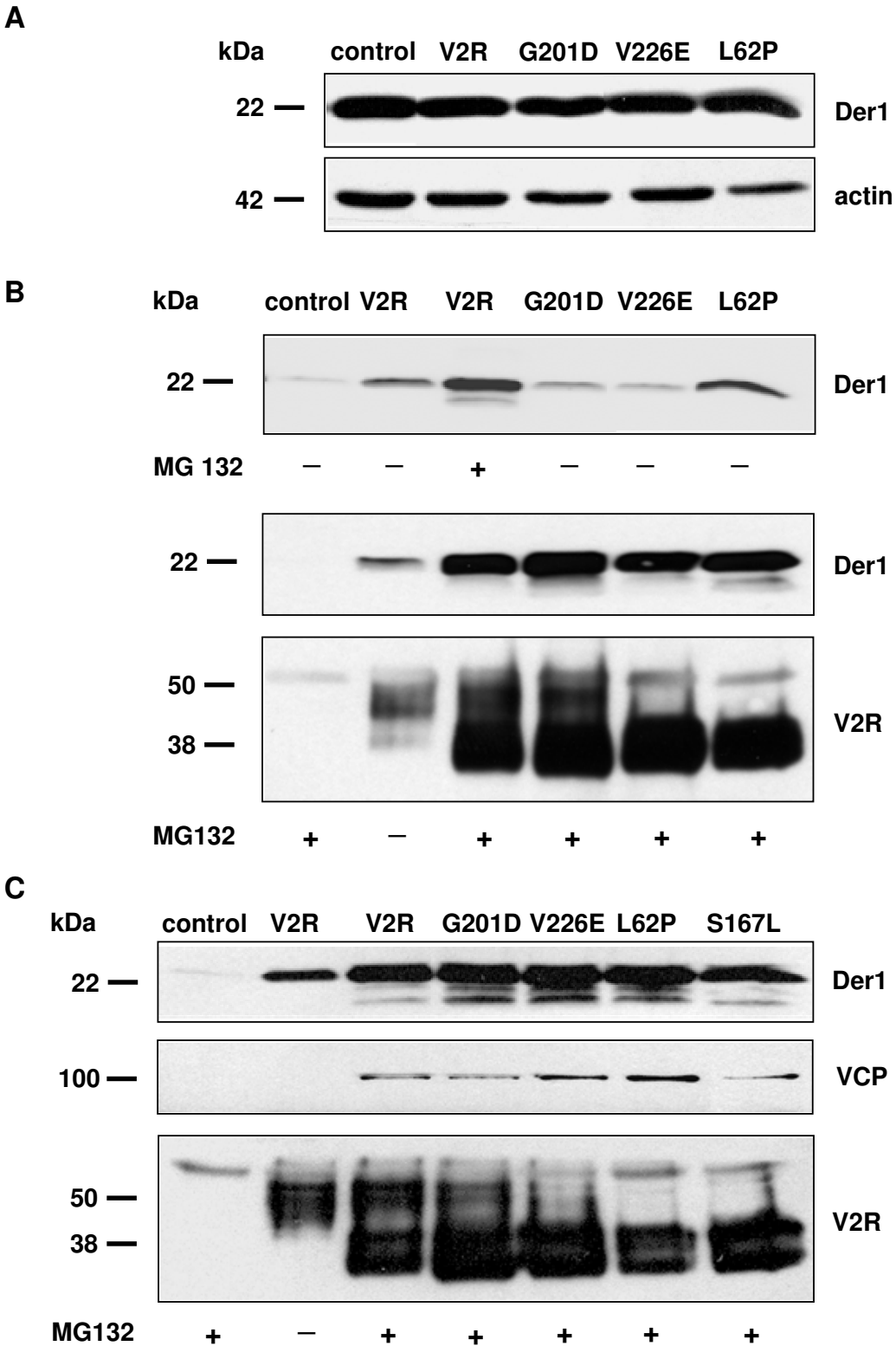

Fig. 19: Interaction of the V2R and NDI-causing mutants with Derlin-1. *A*, total cell lysates of HEK293 cells analyzed for Derlin-1 expression levels by western blotting are shown in the top panel. Actin was used as loading control. *B*, wild-type and mutant V2Rs in presence (+) or absence (-) of MG132 were immunoprecipitated and analyzed by western blotting. Detection of co-precipitated Derlin-1 was done with a polyclonal rabbit α-Derlin-1 antibody (*middle panel*). Receptors were detected by a mouse anti-FLAG antibody (*lower panel*). Controls were non-transfected HEK293 cells. *C*, immunoprecipitation study of wild-type and mutant receptors analyzed by SDS-PAGE and western blotting. Co-precipitated p97/VCP and Derlin-1 were probed in the upper panels and the V2Rs were detected by the FLAG-tag in the lower panel. Controls were untransfected HEK293 cells. Representative blots of three independent experiments are shown.

Treatment with the proteasome inhibitor stopped the degradation process and increased the amount of immunoprecipitated receptors and of co-precipitated Derlin-1 in all tested samples. No differences in Derlin-1 expression between the wild-type and mutant receptors with different misfolded domains were determined. The nitrocellulose membrane with samples of MG132-treated co-immunoprecipitations was subsequently stripped to demonstrate that receptors were immunoprecipitated in equal amounts.

To exclude that the Derlin-1-dependent ERAD pathway was only used by V226E (mutation in the fifth transmembrane domain), a second mutant V2R with a mutation in the fourth transmembrane domain, S167L, was tested for its Derlin-1 interaction together with the other mutant receptors (Fig.19, *C*).

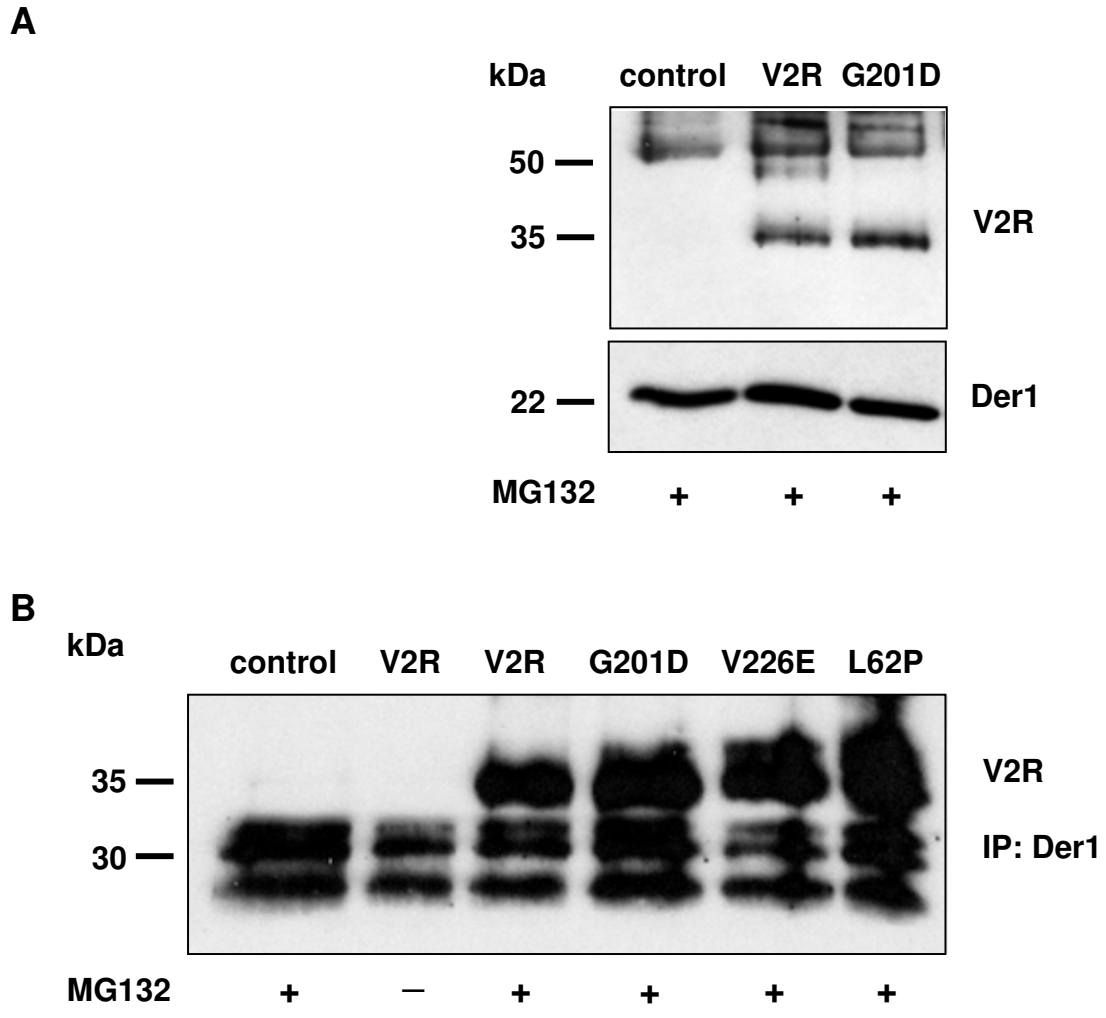

Fig. 20: Reverse co-precipitations: Derlin-1 pull-downs were analyzed for co-precipitated V2Rs. *A*, HEK293 cells stably expressing the wild-type V2R and mutant G201D were lysed and Derlin-1 was immunoprecipitated with an anti-Derlin-1 antibody. Co-precipitated receptors were probed with an anti-FLAG antibody (*upper panel*) and Derlin-1 was detected by an anti-Derlin-1 antibody (*lower panel*). *B*, HEK293 cells stably expressing wild-type V2Rs and indicated mutant receptors were lysed and Derlin-1 was immunoprecipitated with an anti-Derlin-1 antibody. Co-precipitated receptors were probed with an anti-FLAG antibody. Shown are representative blots of three independent experiments.

The S167L mutant was also able to co-precipitate Derlin-1, as a specific band at 22 kDa could be detected. The same was true for p97/VCP, where a specific band at 98 kDa was identified (Fig.19, *C, top and central panels*). Furthermore, no major differences in receptor expression levels between cell clones were detected (Fig. 19, *C*, *lower panel*).

A second control experiment was performed to show that the immunoprecipitation was specific. Antibodies targeted to Derlin-1 were loaded on protein G-Agarose beads and Derlin-1 was immunoprecipitated out of cell lysates from untransfected HEK293 cells, wild-type and G201D expressing cells. After SDS-PAGE and western blot analysis, the co-precipitated, unglycosylated V2Rs were detected at 35 kDa by an anti-FLAG antibody (Fig. 20, *A, upper panel*). Derlin-1 revealed a specific band at 22 kDa after stripping the membrane. The experiment was repeated for all mutants included in the study (Fig. 20, *B*). Derlin-1 pulled down each single mutant, but only in the non-glycosylated receptor form.

The results demonstrate that all tested V2Rs are degraded by one Derlin-1-dependent ERAD pathway, independent of their compartment of intracellular retention and their misfolded domain within the receptor. In contrast to the results determined previously in yeast, only one ERAD pathway seems to be responsible for the degradation of V2Rs with different misfolded domains in a mammalian system.

5.2.6 The E3 ligase Hrd1 is presumably involved in the ubiquitination of V2Rs

E3 ligases facilitate the modification of degradation substrates with 48K-linked polyubiquitin chains. Until now, five different E3 ligases are known to participate in mammalian ERAD: Hrd1, gp78, TEB4, Rma1 and RFP2. Hrd1 is the key enzyme in the ERAD complex of the ERAD-M and ERAD-L pathways described by Carvalho et al. in yeast. Hrd1 is also responsible for ubiquitination of several mammalian dislocation substrates (Kostova, Tsai et al. 2007), therefore this ubiquitin ligase was investigated for co-precipitation with V2Rs. HEK293 cells stably expressing wild-type and mutant V2Rs were lysed and receptor proteins were immunoprecipitated with anti-FLAG affinity gel. Proteins were separated by SDS-PAGE and the co-precipitated proteins were analyzed for the presence of Hrd1. The blot revealed no difference between signals of untransfected HEK293 cells and signals of cells expressing receptor constructs at the expected size of 68 kDa (data in appendix, App. Figure 2). Due to the lack of specificity, the participation of Hrd1 in the ubiquitination of V2Rs cannot be confirmed. Other known ubiquitin ligases of the ERAD pathway could not be tested, because at this time the antibody against Hrd1 was the only which was commercially available. However, E3 ligases that function in ERAD are incompletely characterized and the identification of new E3 ligases will engage the research community in the next decade.

5.2.7 Identification of new interacting proteins in the ERAD pathway of V2Rs

A major outstanding question in the ERAD field concerns the arrangement of all participating proteins into special pathways. To find new interaction partners in the degradation process of the V2Rs, co-immunoprecipitation experiments of wild-type receptors in the presence of MG123 or without proteasome inhibitors were performed and subsequently analyzed by mass spectrometry. After separation by gel electrophoresis, the proteins were stained with Coomassie blue and defined areas of the ubiquitin smear (with MG132) and the negative controls (without MG132) were excised (see the gel in appendix, App. Figure 3) and investigated by nano-esi-MS/MS. The protein sequences found were computed with the SwissProt data system. Interacting proteins are summarized in the following schedules. Table 1 contains the proteins that were co-precipitated without inhibition of the degradation process, only the c-region of the gamma-1 chain of the precipitating antibody (3 peptides, score 147) and the V2R (2 peptides, score 479) were found in the control samples. Proteins that co-precipitated with the V2R in presence of MG132 are listed in table 2.

V2R-associated proteins identified by NanoLC-ESI-MS/MS (without MG132 treatment)

Protein	SwissProt	Molecular mass (*Da*)	Score	Peptides (MS/MS)	Band excised (*kDa*)
Ig gamma-1 chain c region (mouse)	P01869	43359	147	3	200
V2R (human)	P30518	40253	479	2	45
Ig gamma-1 chain c region (mouse)	P01869	43359	63	1	45
Ig gamma-1 chain c region (mouse)	P01869	43359	48	1	35

Table 1: V2R-associated proteins identified by NanoLC-MS/MS in the absence of a proteasomal inhibitor. V2Rs were immunoprecipitated *via* their FLAG tag and separated by SDS-PAGE. Co-precipitated proteins were stained with Coomassie blue, excised from the gel and subjected to in-gel digestion by trypsin. NanoLC-MS/MS experiments were performed and peptides identified in a data-dependent mode (survey scanning) using one MS scan followed by MS/MS scans of the most abundant peak. The most abundant proteins identified are shown.

Many identified proteins are related to cell stress and protein degradation. The highest score yielded the immunoglobulin heavy chain-binding protein (GRP78/BiP); 23 peptides matched with a score of 1399. The chaperone BiP belongs to the heat-shock (Hsp) 70 family and plays an important role in the protein folding process and in the ER quality control system.

V2R-associated proteins identified by NanoLC-ESI-MS/MS (with MG132 treatment)

Protein	SwissProt	Molecular mass (*Da*)	Score	Peptides (MS/MS)	Band excised (*kDa*)
V2R (human)	P30518	40253	426	11	>200
Dynein heavy chain (human)	Q14204	532072	154	5	>200
Desmoplakin (human)	P15924	331569	146	4	>200
V2R (human)	P30518	40253	246	5	200
V2R (human)	P30518	40253	82	1	130
Ig gamma-1 chain C region (mouse)	P01869	43359	46	1	130
Ig gamma-1 chain C region (mouse)	P01869	43359	130	2	100
26S proteasome non-ATPase regulatory subunit 2 (Rpn1)	Q13200	100136	447	9	90
Heat shock protein HSP 90-β (HSP 84)	P08238	83081	390	8	90
Heat schock protein HSP 90-α (HSP 86)	P07900	84476	253	5	90
V2R (human)	P30518	40253	120	3	90
Immunoglobulin heavy chain-binding protein (GRP78/BiP)	P11021	72288	1399	23	70
Heat shock 70 kDa protein 6 (human)	P48741	26890	74	1	70
Elongation factor 1-a1 (eEF1A-1)	P68104	50109	621	13	45
26S proteasome ATPase regulatory subunit 7 (Rpt1/S7)	P35998	48472	352	5	45
V2R (human)	P30518	40253	86	1	45

Table 2: V2R-associated proteins identified by NanoLC-MS/MS in the presence of MG132. V2R samples (incubated for 16 h in presence of MG132) were immunoprecipitated *via* their FLAG-tag and separated by SDS-PAGE. Co-precipitated proteins were stained with Coomassie blue, excised from the gel and subjected to in-gel digestion by trypsin. NanoLC-MS/MS experiments were performed and peptides identified in a data-dependent mode (survey scanning) using one MS scan followed by MS/MS scans of the most abundant peak. A subset of proteins identified is shown; the complete data are listed in appendix.

Moreover, other members of the Hsp 70 and 90 families were pulled down by the V2R (Hsp70 protein 6: 1 peptide, score 74; Hsp90-α: 5 peptides, score 253; Hsp90-β: 8 peptides, score 390). Heat-shock proteins are constitutively expressed under basal conditions; in response to cell stress their expression is up-regulated. They have various cellular functions; the best known are their assistance in protein folding and attenuation of aggregation of misfolded proteins.

Furthermore, the 26S proteasome non-ATPase regulatory subunit 2 (Rpn1) (9 peptides, score 447) and the 26S proteasome ATPase regulatory subunit 7 (Rpt1) (5 peptides, score 352) were detected in MG132-treated V2R samples. The proteasomal subunits belong to the regulatory particle of the 26S proteasome that functions in recognition, deubiquitination and unfolding of dislocation substrates. Elongation factor 1-A1 (eEF1A-1) (13 peptides, score 621) was previously reported to participate in proteasomal turnover by Gonen et al. (Gonen, Smith et al. 1994). Suzuki et al. recently demonstrated chaperone activity for the bovine EF-Tu, the mitochondrial homolog of eEF1A-1. Additionally, the c-region of the gamma-1 chain of the precipitating antibody (4 peptides, score 206) and the V2R (1 peptide, score 86) were identified in the samples (these proteins were also excised off bands of the same size of control samples, see table 1). Desmoplaktin was also detected (4 peptides, score 146), a protein enriched in desmosomes. The dynein heavy chain was found (5 peptides, score 154); the protein functions in microtubuli-associated retrograde transport of cargo vesicles from the plasma membrane to a region near the nucleus.

Many proteins that may participate in the ER- and cytoplasmic quality control system including the ERAD pathway of V2Rs were identified. It is clear that this sensitive method only provides a hint for interesting binding partners and that the results have to be confirmed by other methods.

5.2.8 Analysis of the interaction between the V2Rs and the regulatory subunit Rpt1 of the 26S proteasome

The unknown mechanism of dislocation substrate recognition by the 26S proteasome is an interesting open question in the ERAD field. 48K-linked polyubiquitin chains may not be the only target signal because some substrates without ubiquitin modifications are also described to be degraded by the 26S proteasome (Hoyt and Coffino 2004). In MS experiments, two different subunits of the regulatory particle of the proteasome that interact with the V2R were identified: the 26S proteasome non-ATPase regulatory subunit 2 (Rpn1) and the 26S proteasome ATPase regulatory subunit 7 (Rpt1). The regulatory particle ATPases are assumed to play a role in recognition and membrane extraction of ERAD substrates and also seems to display chaperone activity (Braun, Glickman et al. 1999), so the interaction of V2Rs with Rpt1 was investigated.

Whole cell lysates of the stably expressing cell lines (V2R and mutant receptors, controls were untransfected HEK293 cells) were tested on endogenous expression of Rpt1 by western blot analysis and revealed a specific immunoreactive band at 48 kDa in all samples (Fig. 21, *A*, *upper panel*).

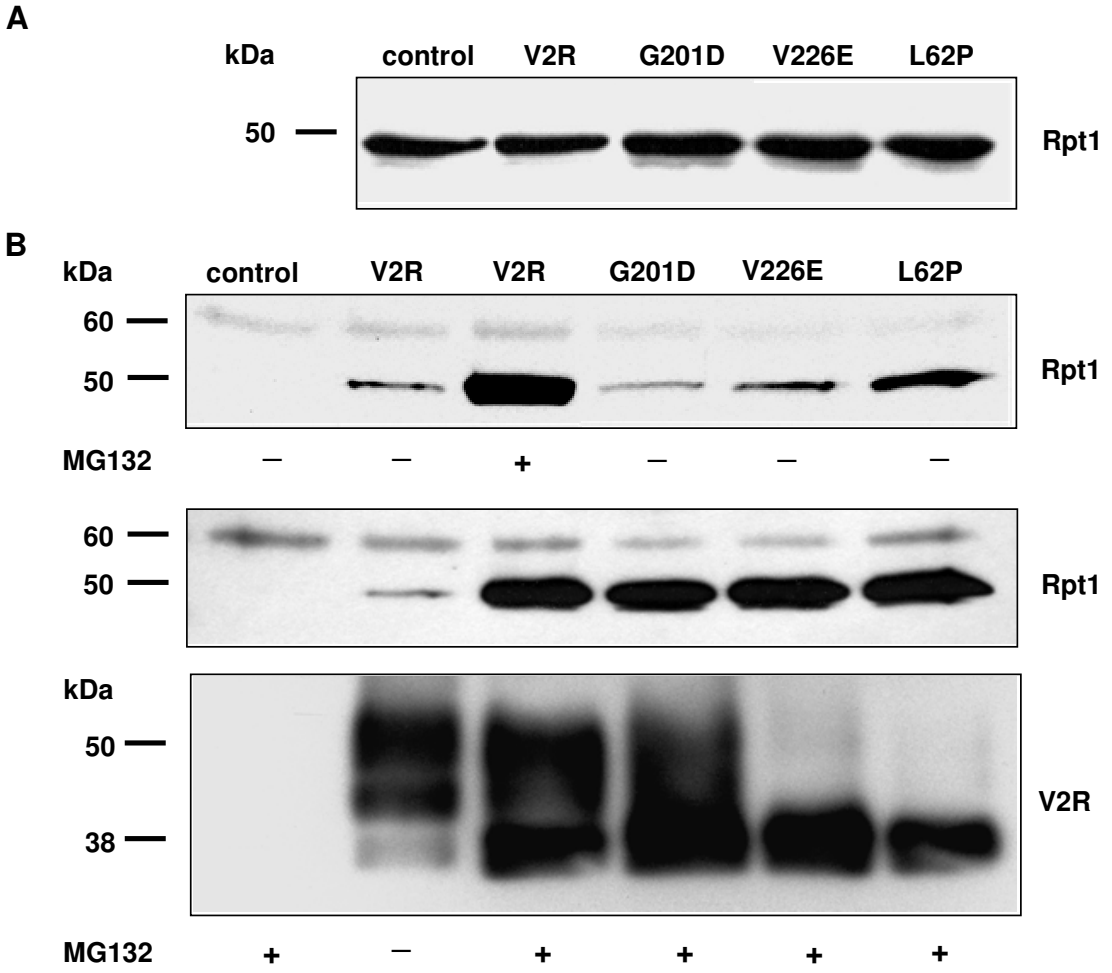

Fig. 21: Interaction with Rpt1. *A*, total cell lysates analyzed for Rpt1 expression levels by western blotting (top panel). *B*, immunoprecipitations of FLAG-tagged V2R wild-type and mutant receptors pretreated with (+) or without (-) MG132 were performed and analyzed by immunoblotting in the two lower panels. Detection of co-precipitated subunits of the 26S proteasome was done with a polyclonal rabbit α-Rpt1/S7 antibody and a POD-conjugated α-rabbit antibody. Controls were non-transfected HEK293 cells. Receptors were detected by a mouse anti-FLAG antibody (*lower panel*). Data are representative of four independent experiments.

Receptors were immunoprecipitated with anti-FLAG affinity gel, separated by SDS-PAGE and co-precipitated regulatory subunits were identified with an anti-Rpt1 antibody (Fig. 21, *B*, *top and middle panel*). Samples without incubation with proteasome inhibitors showed weak, but specific bands of Rpt1 detectable at 48 kDa for all V2Rs; the control sample revealed no specific immunoreactive band. Mutant L62P co-precipitated more Rpt1 then the other receptors under these conditions. As expected, a striking increase in the intensity of the specific band could be observed when cells were

treated with MG132. The receptors were expressed in equal amounts as indicated by development of the stripped membrane with anti-FLAG antibodies (*lower panel*).

5.2.9 V2Rs show no interaction with the regulatory subunit Rpn10

The proteasomal regulatory subunits Rpt1 and Rpn10 are both described to interact with polyubiquitinated proteins (Raasi and Wolf 2007). Binding of subunit Rpt1 to the ERAD complex of the V2R was demonstrated in the present work. Immunoprecipitated V2Rs were also tested for co-precipitation of Rpn10, but the second regulatory subunit was not detectable at 45 kDa (data in appendix, App. Figure 4). This raises the possibility that V2Rs precipitate not the complete multi-subunit regulatory particle, but single components. Furthermore it was of interest if only the regulatory subunits or the complete proteasome was pulled down by the receptors. A mixture of antibodies against different α / β subunits of the catalytic core was tested on whole cell lysates, but failed to detect specific signals (data in appendix, App. Figure 5). Therefore, it could not be confirmed whether V2Rs co-precipitate single regulatory subunits or the complete multi-subunit protease.

5.2.10 Immature V2Rs are retrotranslocated into the cytosol

ER-luminal located ERAD substrates have to be released into the cytoplasm prior to degradation by the proteasome. According to studies of the cystic fibrosis transmembrane conductance regulator (CFTR), ERAD substrates localized in the ER membrane have also to be extracted out of the bilayer into the cytosol before proteasomal turnover (Bebok, Mazzochi et al. 1998). On the basis of these findings, a cell fractionation method was applied to investigate the site of turnover for the V2Rs.

The experiment was performed with untransfected HEK293 cells and cell lines stably expressing wild-type V2R and mutant L62P. Cytosolic and membrane fractions were isolated with the Qproteome Cell Compartment kit from Qiagen (Fig. 22, *A*). Equal amounts of proteins were subjected to SDS-PAGE and immunoblot analysis and the purity of both fractions was controlled by detection of GAPDH (cytosolic marker) and calnexin (ER membrane marker) in both fractions. The receptors were identified by anti-FLAG antibodies. The control cells revealed three prominent unspecific bands in the cytosolic fraction. The western blot of mutant L62P showed only specific bands in the cytosolic (c) and membrane fractions (m) of MG132-treated cells. In the cytosolic fraction, the non-glycosylated receptors were detected at 35 kDa, which implicates retrotranslocation from the ER membrane into the cytosol. In cells without MG132 treatment, the receptors were not detectable anymore, indicating that the proteasome was involved in their degradation.

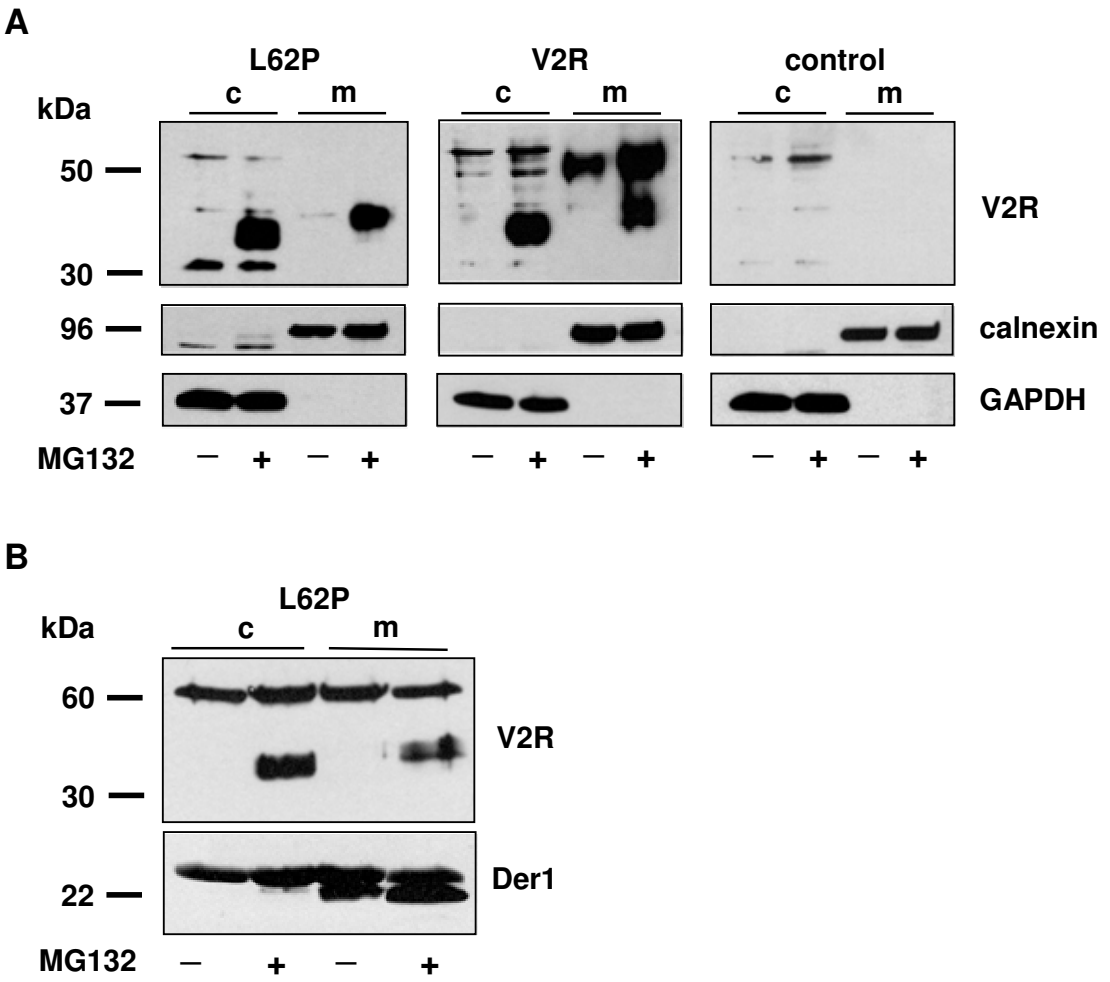

Fig. 22: Cellular fractions analyzed for V2R expression. *A*, HEK293 cells stably expressing wild-type V2R and mutant L62P were either treated with 20 µM MG132 for 16 h (+) or left untreated (-). Isolated cytosolic (c) and membrane (m) fractions were analyzed by SDS-PAGE and immunoblotting. Detection of FLAG-tagged V2R constructs was done with a monoclonal mouse M2 α-FLAG antibody and a POD-conjugated α-mouse antibody. Controls were non-transfected HEK293 cells (control). The purity of cell fractions was confirmed by the detection of calnexin and GAPDH in all isolated fractions. Data are representative of three independent experiments. *B*, Isolated cytosolic (c) and membrane (m) fractions of HEK293 cells stably expressing mutant L62P with (+) or without (-) MG132 treatment were subjected to immunoprecipitation with anti-FLAG affinity gel and analyzed by SDS-PAGE and western blot. Receptors were detected with an anti-FLAG antibody and co-precipitated Derlin-1 was identified at 22 kDa by an anti-Derlin-1 antibody. The 60 kDa and 24 kDa bands were due to the precipitating antibodies.

The membrane fraction of mutant L62P expressing cells revealed an immunoreactive band at 38 kDa corresponding to the core-glycosylated receptors only detectable in presence of MG132. The separated distribution of non- and core-glycosylated receptors in cytosolic and membrane fractions, respectively, clearly shows the deglycosylation of ERAD substrates when retrotranslocated. For the wild-type receptor a similar pattern could be recognized in the cytoplasmatic fraction; only non-glycosylated receptors were apparent in MG132-treated cells. In the membrane fraction, a specific band of 45 – 55 kDa was identified corresponding to complex-glycosylated receptors and was not affected by proteasome inhibition. The core-glycosylated receptors in this fraction could only be detected at 38 kDa in cells treated with MG132. Additionally, a second 35 kDa

band appeared in this fraction that may be due to inefficient extraction out of the membrane. However, in cells with a functional ERAD, no immature receptor forms were detectable. The blots revealed no detectable high molecular mass receptor forms that would be present if the receptors are still ubiquitinated.

In an attempt to obtain more insight into the mechanism of ERAD, the cytosolic and membrane fractions of cells expressing mutant L62P were subjected to immunoprecipitation with anti-FLAG affinity gel (Fig. 22, *B*). In the cytosolic fraction, the non-glycosylated receptor form of L62P was detectable, whereas the core-glycosylated form was restricted to the membrane fraction. In both membrane fractions of cells pre-incubated with or without MG132, Derlin-1 was pulled-down of the whole cell lysates. In contrast, no Derlin-1 could be co-precipitated with receptor proteins of the cytosolic fraction. The Derlin-1 band of the membrane fraction containing accumulated receptor proteins was of higher intensity.

These data support the idea of de-glycosylation of transmembrane proteins after retro-translocation into the cytosol, because glycosylated receptor forms were restricted to the membrane fractions. The receptors further seem to be deubiquitinated and are only detectable in cytosolic fractions after blocking of proteasomal turnover.

5.2.11 Characterization of the influence of polyubiquitinated V2Rs on co-precipitation of phosphodiesterase isoform 4 (PDE4)

It has been shown that phosphodiesterases are recruited upon agonist activation of GPCRs. These enzymes are the counterparts of adenylyl cyclases and degrade the second messenger cAMP arresting cAMP-mediated signal transduction. The β_2-adrenoceptor (β_2AR) interacts with PDE4 isoforms in complex with β-arrestins during desensitation (Li, Huston et al. 2006). The group of M. Houslay demonstrated a similar interaction with a 100 kDa PDE4 for the activated V2R (unpublished results). Furthermore, both receptors are described to be ubiquitinated during the internalization process (Shenoy, McDonald et al. 2001; Martin, Lefkowitz et al. 2003), as well as their scaffolding protein β-arrestin2 (Shenoy and Lefkowitz 2005). To analyze the role of ubiquitination in relation to PDE4 recruitment, V2Rs were isolated by immunoprecipitation with anti-FLAG affinity gel from HEK293 cells in presence or absence of AVP or the proteasome inhibitor MG132 (Fig. 23). Samples were separated by SDS-PAGE and co-precipitated PDE4s were detected with a polyclonal, sheep PDE4 antibody.

Control cells (untransfected HEK293 cells) revealed four unspecific bands depicted by stars (120 kDa, 100 kDa, 30 kDa, 27 kDa). In cells containing the FLAG-tagged wild-type V2Rs, a weak band appeared at 99 kDa, which was slightly enhanced during stimulation with AVP (triangle).

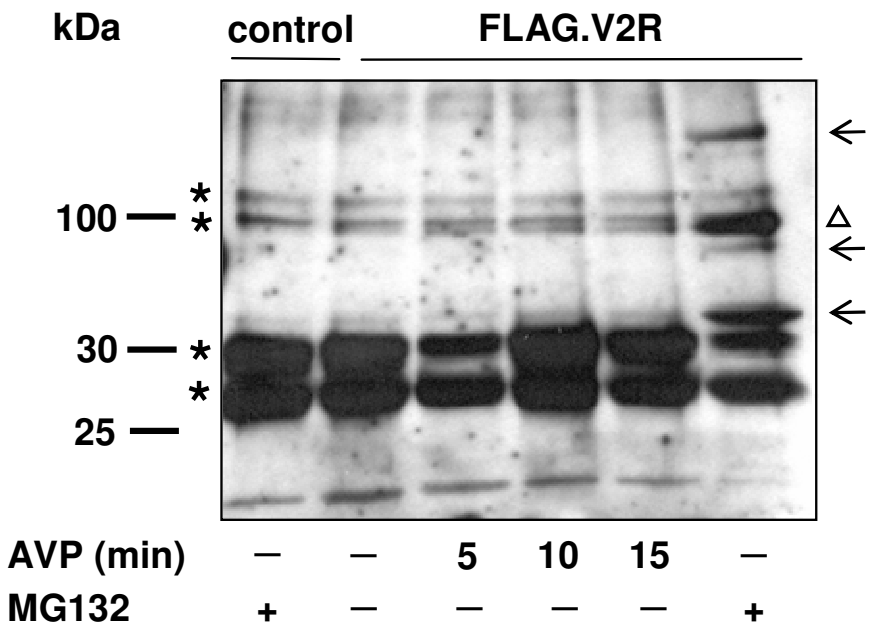

Fig. 23: Interaction of V2Rs with PDE4. HEK293 cells stably expressing the wild-type V2R were either treated with 20 µM MG132 for 16 h (+) or left untreated (-) and were challenged with AVP for indicated times. Controls were untransfected HEK293 cells. Immunoprecipitation of receptor proteins was carried out with anti-FLAG affinity gel and co-precipitated receptor proteins were detected with a sheep anti-PDE4 antibody. Unspecific bands are depicted by stars and PDEs are marked by triangle or arrows, respectively.

Surprisingly, in presence of MG132, a strong increase of the 99 kDa band was detectable and additionally a high molecular band at 150 kDa and two smaller PDE4-corresponding bands at 85 kDa and 35 kDa co-precipitated (arrows). These results indicate that accumulation of immature ubiquitinated and non-ubiquitinated V2R forms facilitates recruitment of different PDE4 subtypes.

Until now, it is not clear if MG132 also influences receptor ubiquitination at the plasma membrane. The functional role, if there is any, of the PDE / V2R interaction remains to be elucidated. However, this experiment clarifies the extensive changes in signal transduction due to modification of receptors by ubiquitin.

In summary, it was shown that the intracellular quality control system regulates the fate of V2Rs. Mature wild-type and mutant receptors, which are able to escape the quality control system of ER and ERGIC, are degraded in lysosomes. Immature core-glycosylated receptors are excluded from lysosomal turnover. Instead, the core-glycosylated receptors, wild-type as well as mutants, are localized in or transported back to the ER for ER-associated degradation. In the presence of the proteasome inhibitor MG132, the receptors are polyubiquitinated, extracted out of the ER membrane and de-glycosylated in the cytosol. All V2Rs, independent of their misfolded domain within the receptor, interact with the AAA ATPase p97/VCP, the putative ER-translocation channel Derlin-1 and the proteasomal regulatory subunit Rpt1. In contrast to the three independent ERAD pathways described for proteins with mutations in cytosolic, trans-

membrane or ER-luminal domains in yeast, it could be demonstrated that only one Derlin-1 / p97/VCP dependent ERAD pathway facilitates the degradation of V2Rs in a mammalian system.